University of Cape Town

Masters Thesis

Achieving baseline states in sparsely connected spiking-neural networks

stochastic and dynamic approaches in mathematical neuroscience

Author:
Alexander Antrobus

Supervisor:
Associate Professor Jeff Murugan
Co-Supervisors:
Dr. Jonathan Shock
Professor Emeritus George Ellis

A thesis submitted in fulfilment of the requirements
for the degree of Master of Science

in the

Department of Mathematics and Applied Mathematics

July 2015

Declaration of Authorship

I, Alexander Antrobus, declare that this thesis and the work presented in it are my own. I confirm that:

- This work was done wholly or mainly while in candidature for a research degree at this University.
- Where any part of this thesis has previously been submitted for a degree or any other qualification at this University or any other institution, this has been clearly stated.
- Where I have consulted the published work of others, this is always clearly attributed.
- Where I have quoted from the work of others, the source is always given. With the exception of such quotations, this thesis is entirely my own work.
- I have acknowledged all main sources of help.
- Where the thesis is based on work done by myself jointly with others, I have made clear exactly what was done by others and what I have contributed myself.

Signed: _____

Date: _____

UNIVERSITY OF CAPE TOWN

Abstract

Faculty of Science
Department of Mathematics and Applied Mathematics

Master of Science

Achieving baseline states in sparsely connected spiking-neural networks stochastic and dynamic approaches in mathematical neuroscience

by Alexander Antrobus

Networks of simple spiking neurons provide abstract models for studying the dynamics of biological neural tissue. At the expense of cellular-level complexity, they are a frame-work in which we can gain a clearer understanding of network-level dynamics. Substantial insight can be gained analytically, using methods from stochastic calculus and dynamical systems theory. This can be complemented by data generated from computational simulations of these models, most of which benefit easily from parallelisation. One cubic millimetre of mammalian cortical tissue can contain between fifty and one-hundred thousand neurons and display considerable homogeneity. Mammalian cortical tissue (or "grey matter") also displays several distinct firing patterns which are widely and regularly observed in several species. One such state is the "input-free" state of low-rate, stochastic firing. A key objective over the past two decades of modelling spiking-neuron networks has been to replicate this background activity state using "biologically plausible" parameters. Several models have produced dynamically and statistically reasonable activity (to varying degrees) but almost all of these have relied on some driving component in the network, such as endogenous cells (i.e. cells which spontaneously fire) or wide-spread, randomised external input (put down to background noise from other brain regions). Perhaps it would be preferable to have a model where the system itself is capable of maintaining such a background state? This a functionally important question as it may help us understand how neural activity is generated internally and how memory works. There has also been some contention as to whether "driven" models produce statistically realistic results. Recent numerical results show that there are connectivity regimes in which Self-Sustained, Asynchronous, Irregular (SSAI) firing activity can be achieved. In this thesis, I discuss the history and analysis of the key spiking-network models proposed in the progression toward addressing this problem. I also discuss the underlying constructions and mathematical theory from measure theory and the theory of Markov processes which are used in the analysis of these models. I then present a small adjustment to a well known model and provide some original work in analysing the

resultant dynamics. I compare this analysis to data generated by simulations. I also discuss how this analysis can be improved and what the broader future is for this line of research.

Acknowledgements

The author would like to thank Associate Professor Jeff Murugan, Dr Jonathan Shock and Professor Emeritus George Ellis for supervising and encouraging this work.

Thank you to the University of Cape Town Postgraduate Funding office for partially supporting me during my Masters.

Thanks to Dr Marc-Oliver Gewaltig for setting me on the path to this project and introducing me to most of the relevant literature.

To all those who attended and engaged in my regular seminars on mathematical neuroscience, thank you for the enthusiasm.

To my parents, thank you for always supporting me in any and all ways. It never goes unnoticed.

Contents

List of Figures

List of Tables

Notes, Terms and Abbreviations

L-I-&-F of **LIF**	**L**eaky **I**ntegrate-and-**F**ire (neuron)
H-H	**H**odgkin-**H**uxley model
Pr{}	**Pr**obability of the observable in braces occurring.
In Vivo	Latin:"*within the living*" – to take place in the living subject.
In Vitro	Latin:"*in glass*" – to take place in the extracted/artificially grown sample.
CV	**C**oefficient of **V**ariation: $CV = \frac{\sigma}{\mu}$.
ISI	**I**nter **S**pike **I**nterval.
Afferent / **Efferent**	An **afferent** neuron sends spikes to its **efferent** neurons.
Links	Links to websites are coloured grey.
BM	**B**rownian **M**otion.

Chapter 1

Introduction

It has long been known that, perhaps in its crudest form, the brain can be thought of as a "mass of excitable units", each receiving and giving input to other units [Beurle, 1956]. This line of thought has developed fruitfully over the past five decades into an approach to theoretical neuroscience based firmly in dynamical systems theory. From single neuron models, theoreticians can conceptualise and, to within the bounds of complexity, simulate clusters of neurons interacting. It is widely accepted that neural function, or information processing, occurs predominantly at this "micro-network" level [Mountcastle, 1957] [Arbib, 2003, p. 31]. To try and understand the basis of information processing in neural tissue we need to understand the dynamics of brain-like networks. The ease of doing so mathematically obviously depends on the complexity and degree of homogeneity of our chosen network model, as well as on our choice of parameterisation. As is always the case in mathematical modelling of a "real" system, we have a trade-off between degree of complexity (how many variables and parameters of the real system are present in the model) and ease of analysis.

We can distinguish between two (of many) subjects in neurodynamics along the lines of single cell models and network models. The former began in earnest with the research of Alan Hodgkin and Andrew Huxley. Their Hodkgkin-Huxley (H-H) model constitutes a framework which can potentially "fit" any biological neuron we currently know of, by adding relevant ion channels and relevant models for synaptic exchange[1]. In electro-physiological dynamics of nerve cells, the principle quantity of interest is V - the potential difference across the cell membrane. This quantity depends on the relative concentrations of various charged ions (principally potassium

[1] Of course, the literature describes various mechanisms beyond the traditional H-H framework but many of these are either rarely observed or readily implemented as extensions of the H-H model.

and sodium) on either side of the cellular membrane. Hodgkin and Huxley's work consisted of analysing the system of ordinary differential equations which described how the local membrane potential coupled to the local flow of potassium and sodium ions through the membrane (see figure 1.1). This flow is controlled by ion-channels embedded in the membrane. These ion channels can change shape, opening and closing, to control the flow of ions. Their shape has a non-linear dependence on the membrane potential. Hodgkin and Huxley used numerical phase-plane analysis to show that, in their model, there exists a "critical value" for V at which the ion-channels open/close rapidly, causing a sudden fast rise (spike) in V (which propagates down the axon) before it returns to the stable fixed-point value. Spikes are principally observed on axons and initiate at the point where the axon meets the cell body, or soma - called the *axon hillock* [Arbib, 2003]. For an extremely engaging introduction to these results in a mathematically rigorous setting, see [Scott, 2002].

The H-H model is, in its simplest form and without considering dendritic or axonal geometry, a system of considerable complexity. Numerical modelling of small networks of H-H based neurons is now easily facilitated by software like NEURON but any form of analysis to derive global dynamics of these networks and larger network models is not possible. A wide variety of simpler neuron models are thus implemented, some derived from the H-H system, others built phenomenologically. The concept of the "leaky integrate-&-fire" (LIF) neuron is built phenomenologically from the H-H results: treating the neuron as a point particle, we do not consider any geometry to the cell. A spike is a "Yes/No" occurrence[2]. More detail is explained in section 1.2 and section 2.1.

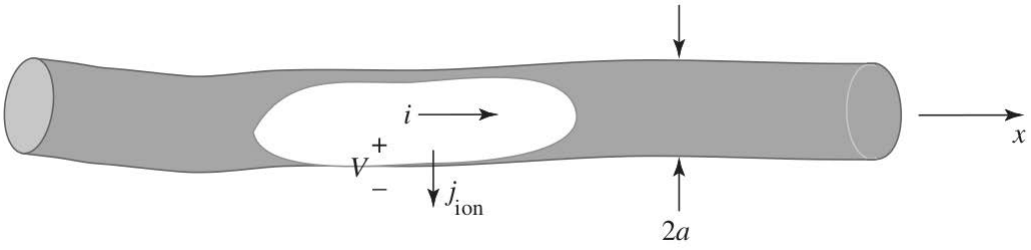

FIGURE 1.1: Nerve Axon. Spikes (or action potentials) propagate principally down the axons of nerves to synapses, where they cause the release of synaptic vesicles which, in tern, cause an influx of charged ions in/out of the post-synaptic neuron, effecting its membrane potential. This diagram shows a schematic representation of the axon, with V labelling the membrane potential. j_{ion} denotes the flow of ions which changes the membrane potential locally. i denotes the resultant longitudinal flow of currents due to the fact that V will vary from point to point along the length of the axon (x-axis). Taken from [Scott, 2002].

[2]We do know, though, that this is not in fact the case. Thresholds are dynamic. For an interesting discussion, see [Mitry et al., 2013]

The term "spiking-network model" refers to networks in which distinct neurons emit spikes, as opposed to networks where only rates of network populations are considered (like Wilson-Cowan models [Wilson and Cowan, 1973]), or networks where "neurons" are discrete computational devices - like perceptrons [Public, 2014]. Of course, as mentioned above, the model used to exhibit spiking behaviour can differ considerably in structure and complexity, from H-H-like models to L-I-&-F models.

Such spiking-networks are often seen computationally as attractor neural networks. This means that a computation is seen to be the process of the network settling into a dynamic state (output of computation) - an attractor of its dynamics - given a certain initial state (input to computation). In particular, this mechanism has been welcomed as a strong candidate for very short-term, or *working* memory [Amit and Brunel, 1997, Barbieri and Brunel, 2008].

Transitions between such states can occur due to external inputs. Changes in the distribution and nature of the attractors (bifurcations) comes about through changes in parameterisation - usually connectivity or external input. An interesting field of research is how the large time-scale dynamics of parameter evolution (learning) relates to the small time-scale dynamics of the network, since both depend on the same input! Before this can be considered, though, there is the simple milestone of whether these models are *capable* of maintaining the dynamic regimes observed in living tissue. In particular, mammalian cortical tissue is almost never silent. Even in unconscious specimens, and across several species, an observed section of cortical tissue can be expected to display spiking. In particular, a dynamic state of random, low-rate firing is commonly observed in tissue which is not receiving any task or sensory specific input [Latham et al., 2000]. This background state can be best understood as follows: if an arbitrary neuron in such a section of cortex was observed, we would find that its spiking activity well described by a Poisson process, with mean rate $\lambda \sim 1 - 5$ Hz, interspersed with short periods in which the neuron may "burst" - firing repeatedly and rapidly.

A standard requirement for any spiking network which claims to simulate cortical dynamics is to reproduce this basal activity state. Several have endeavoured to do so and claimed some success [Latham et al., 2000, Brunel, 2000], though, to my knowledge, all require some form of driving, or external input. This is usually in the form of excitatory cells which fire spontaneously (endogenous cells) or in the form of input coming into some/all cells from "excitatory neurons outside the network" [Brunel, 2000]. Mathematically, these amount to essentially the same thing: an imperfection parameter (as will be shown later). Perhaps it would be preferable

if the network could maintain dynamic activity itself while still within reasonable parameter regimes? There are several reasons for this; the first is that maintaining (localised) neural activity, without external stimulus, is a promising candidate for how short-term memory works. Secondly, it may help us to understand how brains remain active during states when external stimuli are seemingly absent (unconsciousness, sleep). Thirdly, we all know intuitively that a significant amount of our thoughts are seemingly generated from "within", suggesting neural systems must have significant means of generating and maintaining activity without external inputs. The recently released simulation results in [Gewaltig, 2013] suggest that this is possible.

Mathematical neuroscience applies various disciplines of mathematics in investigating questions in neuroscience. When considering models of spiking neurons, techniques used come from non-linear dynamics theory, stochastic calculus and the study of stochastic processes. It is assumed the reader has a good grasp of basic dynamical systems theory: theory of bifurcations and stability analysis. If not, all relevant information can be found in [Strogatz, 1994]. An extremely brief but fairly thorough introduction to stochastic integrals (and the underlying measure theory) appears in appendix A as the author found it beneficial to teach himself this during the preparation of this work. The other appendices contain various constructions and derivations used in the analysis.

The rest of this thesis is laid out as follows. The rest of this Introduction discusses early attempts to model cortical activity, mentioning key developments in the literature and ultimately introducing the L-I-&-F based "Brunel Model" of sparse, weakly connected networks of excitatory and inhibitory neurons. In the Results section, some of the published analysis of this model are presented, particularly where it pertains to sustainability and spiking statistics of low-rate activity. Thereafter I discuss some original, preliminary results from analysing and extended form of the Brunel model which was inspired by the numerical results in [Gewaltig, 2013]. In chapter 3 I compare some predictions from this new analysis to results from multiple simulations. In chapter 4 I review the main points to be taken from this text and discuss how it relates to current research in theoretical and computational neuroscience.

1.1 Neural tissue as a mass of threshold units

Richard Beurle, followed by Ross Ashby, Heinz Von Foerster and Crayton Walker [Ashby et al., 1962], were some of the earliest authors to consider the dynamics of structures with "properties

similar to those of neurons" [Beurle, 1956]. Beurle found that, in a homogeneous plane of excitable cells with some proximity dependent connectivity distribution, any type of global, stable activity was inherently unstable but that one could expect waves of activity to propagate (possibly repeatedly) across the mass. Ashby et al. then proposed a model where they derived a function for the probability of a unit emitting an output spike given the probability of its afferent units emitting input spikes. This results in a binomial distribution in the mean firing probability and, using this as an iterative map, they supplied a more rigorous proof that low or intermediate rate firing activity is inherently unstable for this system of recurrently connected, excitatory threshold units. They concluded that "the more richly organised regions of the brain offer us something of a paradox." Griffiths showed in 1963 that just such a paradox could be overcome with the introduction of inhibitory units to the system [Griffith, 1963]. To be more explicit, consider a homogeneous (near infinite) mass of identical "excitable" units. We choose to observe one specific unit. This unit has C_e excitatory and C_i inhibitory incoming connections (as do all other units) and it and may receive as many as n_e ($C_e \geq n_e \geq 0$) excitatory and n_i ($C_i \geq n_i \geq 0$) inhibitory inputs via these connections during a step of discretised time (Δt). If the number of excitatory inputs minus the number of inhibitory inputs is enough to push the unit beyond the threshold, θ, then the unit will fire. The other units, which send input to this unit, are all identical (save that some cause inhibitory and others excitatory input) and have equal probability of spiking, say p. Let $q = 1 - p$, then q is the probability that an arbitrary unit *does not* fire in a time step. The probability that our observed unit fires within a given time step of discretised time, is then given by

$$\Pr\{\text{neuron spikes}\} = \sum_{n_e - n_i \geq \theta} \binom{C_e}{n_e} \binom{C_i}{n_i} p^{n_e + n_i} q^{C_e + C_i - n_e - n_i}. \tag{1.1}$$

The summation is performed over all possible combinations of (n_e, n_i) which satisfy the condition $n_e - n_i \geq \theta$. The observed neuron is the same as all other neurons though! Hence we expect that $\Pr\{\text{neuron spikes}\} = p$, by definition. We can be plot equation (1.1) as a function of p, or rather a distribution for p and solve visually or numerically for the value p^* such that

$$p^* = \sum_{n_e - n_i \geq \theta} \binom{C_e}{n_e} \binom{C_i}{n_i} (p^*)^{n_e + n_i} (q^*)^{C_e + C_i - n_e - n_i}. \tag{1.2}$$

This is interpreted as the expected fraction of the total population which fired in Δt such that, in the next Δt, the same fraction fire again, et continuum. Griffiths showed that for a small region of parameter space (not too many connections coming in to each unit and carefully

balanced ratios of excitation and inhibition in the network), this system displays a stable fixed point at $p^* = 1/2$. Achieving this, though, requires parameter choices which are unreasonable from a physiological point of view [Gewaltig, 2013]: namely very a small ratio of threshold (θ) to excitatory input strength (J): $\theta/J < 10$. In the above Griffiths model, the excitatory input strength in dimensionless and normalised to 1 but, as is the case for the more biologically plausible models introduced below, excitatory input to a neuron causes a change in its membrane potential (measured in Volts) and could take an arbitrary value. To push the stable value below 0.5 (half the network firing at any given moment, which is not particularly reasonable), we can increase C_e and C_i. The cost is that the probability distribution of p narrows, meaning the network cannot tolerate large fluctuations from the stable state without moving beyond the basin of stability. More importantly, if we consider parameters that mirror what little we *do* know about cortical physiology, namely a large number (∼4-10 000) of connections coming into each node [Braitenberg and Schütz, 1998] we are hard-pressed to find plausible (i.e small p^*) stable states in this model. A more complex, biologically inspired model is that of Amit, Tsodyks, Brunel and others which forms the body of the discussion in this thesis.

Other early theoreticians, like Richard Stein and Henry Tuckwell, looked at how individual neurons process their inputs, or rather, how the statistics of their inputs effect their firing activity [Stein, 1965, Stein, 1967], [Tuckwell, 1976]. The membrane potential of a an individual neuron is treated as a random variable (see appendix B) which obeys a continuous Markov process, or diffusion process and, assuming a simple threshold-fire condition, models were proposed to calculate the efferent firing rates and variabilities, given the parameters of the afferent Wiener process input. Descriptions and derivations of various components of this theory appear in this thesis in appendix B, as they are now routinely used to analyse contemporary network models.

Two decades later, the question of dynamic activity in models of neural tissue received new interest thanks to two key papers [Vreeswijk and Sompolinsky, 1996, Vreeswijk and Sompolinsky, 1998]. In the first Carl Van Vreeswijk and Heim Sompolinsky developed a model in which the Poissonian distributions of individual neurons' spike times depend on fluctuations in their input from a sub-threshold mean. They showed that these spike-time distributions are a result of the deterministic (but chaotic) dynamics of the network, *not* the presence of randomised external input or driving. All of this occurs because there is a balance in the network: average mean inhibition cancels average mean excitation but fluctuations from the mean cause neurons to spike. In this model, each neuron receives, on average, K inputs from each of the three populations: excitatory, inhibitory and external excitatory. The populations are much larger

than the number of connections per neuron, so correlations between inputs are weak. Thus the mean excitatory input to each population is of order K, as is the inhibition, but fluctuations therein are of order $\sqrt{K}$. If the thresholds of neurons are also of order $\sqrt{K}$, they have a reasonable chance of firing. This model also showed is that, where Griffith's model predicted that excitatory and inhibitory strengths need balance quite precisely, in this randomly connected network setting, only the *averages* of excitation and inhibition need balance. Finally, the authors pointed out that although a small increase in the input is not enough to ensure that each neuron fires in the next time step, the chaotic dynamics of individual neurons ensures that, at any moment, enough neurons are near threshold to fire immediately and increase the population rate within a single time step. They propose that this explains how nervous systems can react on time-scales much smaller than those of individual neurons (governed by the membrane time constant). This is an early, simple form of population coding.

The model of Van Vreeswijk and Sompolinsky had two-state neurons and still discretised the dynamics of individual neurons: updating the state of excitatory neurons once every time-step τ and that of inhibitory neurons once every 0.9τ. The state of a neuron at update depends solely on the value of its K inputs at that moment of update. Steps to make this approach more biologically plausible appeared in [Amit and Brunel, 1997], where self-stability in a network of I-&-F neurons was shown to be stable via similar mechanisms but in the more realistic setting of each each neuron having a large number of efferent connections. In this setting, the average membrane potential of an individual neuron sits far away from the defined resting potential. This was called *renormalisation* of the resting potential. Taking things a bit further, Amit and Brunel showed that, by creating local clusters of increased connectivity within the excitatory population and by making these connections stronger, their network could display *selective sustained activity*, a phenomenon observed in delayed response experiments. This means that for non-specific input to the network, the network activity displays statistics similar to those of *in vivo* observed background states. But, with specific, heightened input to these local clusters (target specific input), the clusters would display significantly increased rates ($\sim$ 5 times the background) which were stable even after the specific input was removed. During this time, the rest of the network displayed only slightly elevated rates. Interestingly, the existence of these stable elevated rates depended on the relative strengths of the in-cluster excitatory connections *and* on the out-of-cluster excitatory connections. Only above a specific threshold relation for these values did a bifurcation occur and the localised, increased, stable rates appear.

In dynamical systems theory, these stable activity states are called *attractors* of the phase space,

thus these networks of spiking-neurons which display stable activity states are often referred to as *attractor neural networks*. During working memory tasks, cortical tissue (*in vivo*) displays regions of localised heightened rate activity [Compte et al., 2003]. Thus, as pointed out by Amit and Brunel, localised sub-populations displaying increased activity qualitatively reproduce this phenomenon. Different spiking network models with randomised, sparse connectivity have been quite successful in roughly reproducing the statistics observed in background, non-localised activity[3]. The next question is whether models can reproduce the statistics observed in small populations with heightened rate activity. An interesting discussion of this appears in [Barbieri and Brunel, 2008]. The authors discuss experimental results which suggest the firing dynamics of the selective memory subnetworks are *highly* irregular during active working memory, ($CV_{ISI} > 1$). In contrast, models like those of [Amit and Brunel, 1997, Brunel, 2000] have $CV_{ISI} << 1$ for the selective populations in the high-activity state. This is because in the high activity state, these neurons are being strongly driven by supra-threshold input. Some models have been proposed which take steps toward solving this problem but this is beyond the scope of the current text (see [Barbieri and Brunel, 2008] for references).

1.2 The Brunel model

The model described below was perhaps first introduced in its entirety by Daniel Amit, Misha Tsodyks and Mosha Abeles in the late 1980s and early 1990s. Many aspects of the associated analysis, though, were done in relation to other models, such as that of Stein in 1965 and Tuckwell in 1977. Since the precise formulation I use below comes from the work of Brunel [Brunel, 2000] and Amit and Brunel [Amit and Brunel, 1997], I will refer to it as the "Brunel model".

Consider the following network formulation:

- Single neuron dynamics are given by the L-I-&-F model:

$$\tau \dot{V}_i = -V_i + RI_i, \tag{1.3}$$

where i's index from 1 to N - the total number of neurons. R is the membrane resistance and is assumed to remain constant. τ is the membrane time constant, common to all neurons and defines the integrative "time window" of the network. For example, inputs arriving in a window

[3] though there is still some debate around which models do so best.

$\Delta t << \tau$ can be considered "synchronous" since, between inputs, V decays as $e^{-t/\tau}$ and so will have changed little if $\Delta t/\tau << 1$.

- Of N neurons, N_E are excitatory, N_I are inhibitory, hence $N = N_I + N_E$. In reflection of measurement, the ratio of excitatory neurons to inhibitory neurons in the networks is $N_E/N_I = 4$. Excitatory (inhibitory) neurons can only cause positive (negative) changes in the membrane potential of their afferent neurons

- Each neuron receives connections from C other neurons. Of these connections, C_E come from excitatory neurons and C_I from inhibitory neurons. The specific C_E/C_I neurons are determined randomly (i.e. chosen from a square distribution over each population, each neuron being equally likely). Autoconnections are not allowed.

- In addition, each neuron receives C_E external connections[4], simulating input from remote cortical regions. Input on each such connection is an independent Poisson process. All these processes have the same, fixed rate: ν_{ext}. Note, the subscripts $_{ext}/_{int}$ will be used to denote all parameters pertaining to external/internal inputs or activity.

- If a neuron spikes at time t_0, its efferent neurons will receive input at time $t_0 + D$, where D is a uniform delay across the network, approximating for axonal and dendritic delays.

- Connections from an excitatory neuron to any neuron give an input of strength J. Those from inhibitory neurons have input strength $-gJ$. We call g the *inhibitory gain*.

- The initial (resting) membrane potential for each neuron is V_r. If the membrane potential reaches the threshold value, V_θ, the neuron "spikes" (i.e. all its efferent neurons will receive an input D later). Immediately after spiking, the neuron membrane potential is reset to V_r, where it remains *fixed* (impervious to input) for a fixed refraction period, τ_{rp}. At the end of this period, the membrane potential is again dynamic. For purposes of analysis, it is only the ratio $\frac{V_\theta - V_r}{J}$ which defines how easily a neuron fires. Hence, without loss of generality, we will restrict ourselves to the value $V_r = 0$ and hence only V_θ/J is relevant.

[4]This value seems highly variable. As a fraction of all excitatory connections received by a neuron in a microcolumn of cortex, connections from without the column have been found to account for between 20% and 50% of them [Braitenberg and Schütz, 1998]. Here we have the total number of connections per neuron is $C_E(2.25)$, so external connections constitute just under 50%.

We assume that the total potentiation entering a cell soma can be written as the weighted (by J's) sum of firing rates of pre-synaptic neurons, indexed by j:

$$RI_i(t) = \tau \sum_{j}^{C} J_{ij}\nu_j(t - D). \tag{1.4}$$

Note that we are summing here only over the specific C neurons which are pre-synaptic to neuron i. $\nu_j(t - D)$ is the mean firing rate of pre-synaptic neuron j at time $t - D$. This formulation is derived from the more exact treatment of post synaptic currents entering a cell as spike trains (see appendix C).

In the above formalism, excitatory and inhibitory neurons have the same characteristics (membrane time constants, thresholds, delays, etc.), they differ only in the strength and sign of their connection weights. Brunel extended his analysis to include some diversity in these parameters, which we will not consider here.

A key principle in analysis of the Brunel model is **sparse connectivity**, namely that $\frac{C}{N} = \frac{C_E}{N_E} = \frac{C_I}{N_I} = \epsilon << 1$. This said, the number of connections received by each neuron remains large ($\sim 10^3 - 10^4$), as this is what is evident in Biology [Braitenberg and Schütz, 1998]. For this reason, Brunel assumed each individual connection strength to be relatively small compared to the threshold ($\tau J << V_\theta$), otherwise only a few spikes would cause a neuron to fire and the resultant firing rates would be extremely high, like those of the Griffiths model. These assumptions imply a neuron requires a fairly large fraction of near synchronous inputs to reach threshold. Assuming we can extrapolate at least roughly from the Griffiths model, we should not find it surprising that this parameter regime *cannot* display self-sustained activity and hence the networks and analysis considered in [Brunel, 2000] require non-zero external input.

a priori criticisms and shortfalls of the Brunel model

The I-&-F neuron model undoubtedly does not capture the full suit of dynamics evident in cortical neurons. It is stressed, though, that the purpose of the model is to investigate the *emergent* dynamics of the system: dynamics which result from the interplay of excitation and inhibition and from the connectivity of the network. The choice of a simple neuron model offers obvious benefits in this regard: easier and more efficient simulation, easier analysis and confidence in interpretation of dynamics. What I mean by this is that, if a certain dynamic

regime is observed which we *know* is beyond the dynamic repertoire of the a single neuron, we can be confident it is the result of collective dynamics.

The connectivity of the Brunel model is quite reasonable in accounting for local connectivity patterns [Braitenberg and Schütz, 1998]. In particular it is preferable to the simplistic models of Griffiths and others because it reflects the high degree of connectivity (large C) present in the neocortex. It includes synaptic/axonal delays (D) and considers simple single-neuron dynamics. How well it approximates the effects of distal inputs is perhaps debatable, and most significantly, it is wholly negligent of anatomy. Cortex has layered structure, consisting of between three (hippocampus) and six (neocortex) layers [Braitenberg and Schütz, 1998]. Layers are defined predominantly on what cell bodies are contained in the layer, and connectivity between different layers follows definite profiles, for example: *most* connections from L4 go to L5 and L4 and are predominantly inhibitory in nature. *Most* projections from L5 are excitatory and are recurrent to L5, with many others feeding to L4 etc. In absolute numbers, though, the Brunel model captures the prevailing ratio of excitatory to inhibitory neurons in neocortical systems at 4:1.

Chapter 2

Analysis of Brunel and Gewaltig models

In this section I discuss some of the analysis of the Brunel model as described in [Brunel, 2000]. First though, I discuss the L-I-&-F neuron in the Brunel model setting and describe the dynamics of the resultant Langevin equation. Section 2.3 consists of original work in which I make a small adjustment to the Brunel model and provide preliminary analysis on the resultant dynamics.

2.1 Dynamics of the Integrate-and-Fire Neuron

We begin with the expectation that each neuron receives a large number of inputs, each from a different presynaptic cell, with the total number of inputs much smaller than the total number of neurons. This means two arbitrarily chosen neurons are unlikely to share a common source of input and thus should experience essentially uncorrelated input. If we additionally require background activity rates to be low ($\sim$ 5 Hz), we can effectively approximate the input to a single neuron as a Gaussian process. We write[1]

$$RI_i(t) = \mu(t) + \sqrt{\tau}\sigma(t)\eta_i(t) \tag{2.1}$$

[1]See appendix C and [Amit and Brunel, 1997] for details of argument.

where η_i is a white noise process with zero mean and unit variance. For simple reference later, this gives us the Langevin equation[2].

$$\tau \dot{V}_i = -V_i + \mu_i(t) + \sqrt{\tau}\sigma_i(t)\eta_i(t). \tag{2.2}$$

For clarity's sake, we take a brief, qualitative look at the simple dynamics of the above Langevin equation along the lines of [Tuckwell, 1988] and [Gerstner and Kistler, 2002]. Let $X(t) := e^{t/\tau}V(t)$. Then $\dot{X} = \frac{e^{t/\tau}}{\tau}\left(\mu(t) + \sqrt{\tau}\sigma(t)\eta(t)\right)$ for $t > 0$ and

$$X(t) = X(0) + \tau^{-1}\int_0^t e^{u/\tau}\left(\mu(u) + \sqrt{\tau}\sigma(u)\eta(u)du\right).$$

Remember $\eta(t)$ is a random variable and hence this integral is in fact a stochastic one. Nevertheless we can consider the expectation value and variance of $X(t)$:

$$\begin{aligned}\mathrm{E}[X(t)] =& X(0) + \tau^{-1}\int_0^t e^{u/\tau}\mu(u)du \\ \mathrm{Var}[X(t)] =& \tau^{-1}\int_0^t e^{2u/\tau}\sigma^2(u)du\end{aligned}$$

Restricting ourselves to the temporally homogeneous ($\mu(t) = \mu,\ \sigma(t) = \sigma$) case,

$$\begin{aligned}\mathrm{E}[X(t)] =& X(0) + (e^{t/\tau} - 1)\mu \\ \mathrm{Var}[X(t)] =& (e^{2t/\tau} - 1)\frac{\sigma^2}{2}du,\end{aligned}$$

and we easily regain the same values for $V(t)$:

$$\begin{aligned}\mathrm{E}[V(t)] &= e^{-t/\tau}\mathrm{E}[X(t)] = X(0)e^{-t/\tau} + (1 - e^{-t/\tau})\mu, \\ \mathrm{Var}[V(t)] &= e^{-2t/\tau}\mathrm{Var}[X(t)] = (1 - e^{-2t/\tau})\frac{\sigma^2}{2}.\end{aligned} \tag{2.3}$$

It is immediately evident that the mean and variance approach asymptotic limits:
$\lim_{t\to\infty}\mathrm{E}[V] = \mu$ and $\lim_{t\to\infty}\mathrm{Var}[V] = \frac{\sigma^2}{2}$. For $\mu > 0$, we can get some idea of the distribution of escape times from the interval $[V(0), \theta)$ where θ is the firing threshold. If $\mu > \theta$, we can be almost certain the neuron will fire. We can be even more certain if we have that $\mu - \sigma > \theta$ (see figure 2.1). The most interesting scenario though is when $\mu \lesssim \theta$. In this case, it is the statistical

[2]This equation is not very rigorously defined but has become a convention to write down. See appendix A, equation (A.2)

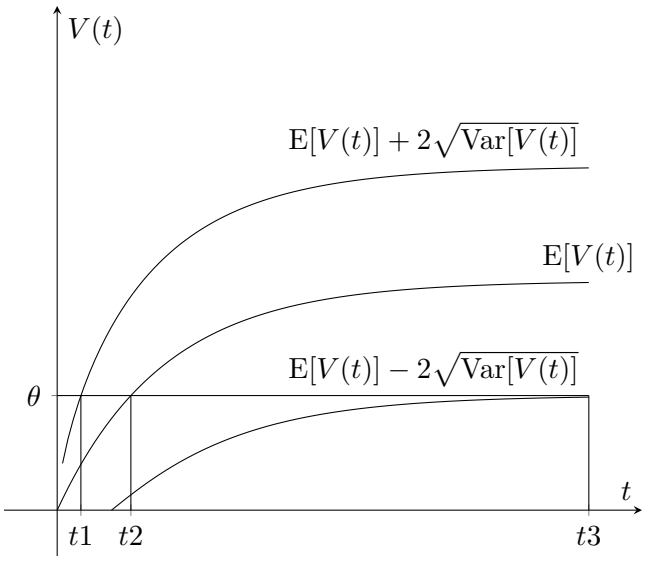

FIGURE 2.1: For positive mean, we can expect that $V(t)$ will reach threshold θ at time $t2$. With even more confidence we can predict that it will reach θ between times $t1$ and $t3$. Calculating $t2$ as a value of the input parameters is trivial but this is not the case for $t1$ and $t3$. For the case of of normally distributed constant input, we expect $\lim_{t\to\infty} V(t)$ to be normally distributed.

fluctuations of the input around the mean which cause the neuron to fire. In particular, suppose $\mu = \theta - \frac{\sigma}{\sqrt{2}}$ and that a neuron has not fired for a "long time" ($t >> \tau$). We can think of $V(t)$ as being in a "steady state", normally distributed around μ. So the probability of finding it in the region $V(t) \geq \theta = \mu + \frac{\sigma}{\sqrt{2}}$ is

$$\lambda = \int_{\mu+\frac{\sigma}{2}}^{\infty} \frac{1}{\sigma\sqrt{\pi}} e^{\frac{(x-\mu)^2}{\sigma^2}} dx.$$

Since $\eta(t)$ is a white noise processes, fluctuations are independent, so the probability of the neuron spiking in the infinitesimally small time interval $[t, \Delta t)$ is roughly $\lambda\Delta t$. For N neurons all experiencing similar (independent) inputs, the total number of spikes from all N is again a Poisson process with rate $N\lambda$. If we have the case that $N >> k$, or that neurons return to the asymptotic state almost immediately (i.e $\frac{1}{\tau} << \lambda$), or that the rate of neurons recovering is also $N\lambda$ (i.e. the system is in a stable state), then we have that the probability of k neurons firing between t and $t + \Delta t$ has a Poisson distribution: $\Pr\{k \text{ in } [t, t + \Delta t)\} = \frac{e^{-N\lambda\Delta t}(N\lambda\Delta t)^k}{k!}$.

2.2 Brunel network in the diffusive limit

Below I will review the analysis from [Brunel, 2000]. This analysis is done in the limit $\frac{C}{N} \to 0$, or that the network is infinitely large. The true mean and variance of the input in the Brunel model

are $\mu(t)$ and $\sigma^2(t)$ respectively. These values will depend on the connectivity, external inputs (ν_{ext}) and global activity of the network (ν_{int}). See appendix C for a description of how these quantities are derived. In the case of the Brunel formulation described earlier, all connections are either excitatory or inhibitory and of fixed relative strengths. From equation (C.4), summing over $C = C_E + C_I = C_E(1 + \gamma)$ connections, (C_E excitatory and $C_I = \gamma C_E$ inhibitory), all active at mean rate $\nu_{int}(t - D)$ we have (similarly for external inputs):

$$\begin{aligned} \mu(t) =& \mu_{ext} + \mu_{int}(t), \\ \mu_{ext} =& C_E J \tau \nu_{ext}, \\ \mu_{int}(t) =& JC_E\tau \cdot (1 - \gamma g)\nu_{int}(t - D), \end{aligned} \tag{2.4}$$

Here the $\cdot$ signifies conventional multiplication of reals. Note that the external input rate is time independent. The *magnitude* of the variance in the input is given by:

$$\begin{aligned} \sigma^2(t) =& \sigma^2_{ext} + \sigma^2_{int}(t), \\ \sigma^2_{ext} =& J^2 C_E \tau \nu_{ext}., \\ \sigma^2_{int}(t) =& J^2 C_E(1 + \gamma g^2)\tau \nu_{int}(t - D). \end{aligned} \tag{2.5}$$

μ_{ext} and σ^2_{ext} denote the mean and variance of the input due to external inputs.

At any moment in time, the individual membrane potentials of the neurons in the system will follow some distribution, labelled $P(V, t)$. P is a distribution over the membrane potentials, V, but a function of time. In specific, when inputs to each individual neuron are essentially uncorrelated, the time-evolution of this distribution obeys a Fokker-Planck equation (for derivation see D):

$$\begin{aligned} \tau \frac{\partial P}{\partial t}(V, t) =& \frac{\sigma^2(t)}{2} \frac{\partial^2 P}{\partial V^2}(V, t) + \frac{\partial}{\partial V}[(V - \mu(t))P(V, t)], \\ & \text{for } V \in (-\infty, V_r) \cup (V_r, V_\theta) \text{ and,} \\ P(V, t) =& 0 \text{ for all } V \geq V_\theta. \end{aligned} \tag{2.6}$$

There is also a refractory probability $p_r(t) = \int_{t-t_{rp}}^{t} \nu_{int}(u)du$, which is the probability that a neuron is refractory at time t and hence its membrane potential is fixed at $V(t) = V_r$ for $t \in [t^*, t + \tau_{rp})$, where t^* denotes the time at which it spiked. So the integral in the expression for $p_r(t)$ is simply counting all neurons which entered the refractory state during the period τ_{rp}

before t.

In a realisation (simulation) of the system, the global firing rate over the interval $[t, t+\delta t)$ is the number of neurons which reach threshold in that time window. Similarly, in the infinitesimal limit, the global firing rate at time t is the rate at which the distribution changes at the threshold. Said differently, the rate at which P flows through the boundary at V_θ is the global firing rate. With this in mind, we define a *probability current* through V at time t as $S(V,t)$, which is then given by

$$\frac{\partial P(V,t)}{\partial t} = -\frac{\partial S(V,t)}{\partial V},$$

The change of sign is to ensure that population rates are positive. Hence,

$$S(V,t) = -\frac{\sigma^2(t)}{2\tau}\frac{\partial P(V,t)}{\partial V} - \frac{V-\mu(t)}{\tau}P(V,t) \tag{2.7}$$

The global, instantaneous firing rate of the network at time t is then given by $\nu_{int}(t) = S(V_\theta, t)$.

2.2.1 Boundary and normalisation conditions

Our statement about the flux of P through the boundary at V_θ, and the fact that a neuron fires instantly upon reaching V_θ (i.e. $P(V,t) = 0$ for $V \geq V_\theta$) implies our first boundary condition at V_θ:

$$\frac{\partial P}{\partial V}(V_\theta, t) = -\frac{2\nu_{int}(t)\tau}{\sigma^2(t)} \tag{2.8}$$

Continuity requirements at the reset potential provide a similar condition; that neurons which fired at time $t - \tau_{rp}$ must have recovered at time t and "re-enter" the system. This provides the following derivative discontinuity:

$$\frac{\partial P}{\partial V}(V,t)\Big|_{V_r^-}^{V_r^+} = -\frac{2\nu_{int}(t-\tau_{rp})\tau}{\sigma^2(t)} \tag{2.9}$$

We also have the natural boundary conditions to guarantee integrability:

$$\lim_{V\to-\infty} VP(V) = 0. \tag{2.10}$$

Finally, normalisation implies:

$$\int_{-\infty}^{V_\theta} P(V,t)dV + p_r(t) = 1 \tag{2.11}$$

2.2.2 Stationary state results

If the dynamics of this network settle into a stationary state, we expect the globally-averaged firing rate to be essentially constant. We can write $\mu_{int}(t) = \mu_{int,0}$, $\sigma_{int}(t) = \sigma_{int,0}$, but the input to each neuron is *not* a fixed, constant function, since different neurons will fire at different time and there may be small fluctuations in the global rate of the network. Since the network parameters are not *evolving* in time, and treat input to each neuron as a temporally homogeneous but stochastic process. We can write this input as

$$IR_i = \mu_{i,0} + \sigma_{i,0}\eta(t), \tag{2.12}$$

where the time dependence in $\eta(t)$ simply means it can have a different value depending at what point in time it is sampled. We make similar substitutions into equation (2.6) and obtain the coupled system

$$\frac{\sigma_0}{2}\frac{\partial^2 P_0}{\partial^2}(V) + \frac{\partial}{\partial}[(V-\mu_0)P_0(V)] = 0,$$
$$p_{r,0} = \tau_{rp}\cdot\nu_{int,0}.$$

Subject to conditions 2.8 and 2.10, a solution to this system is[3]

$$P_0(V) = 2\frac{\nu_{int,0}\tau}{\sigma_0}\mathrm{e}^{-z(V)^2} \times \int_{z(V)}^{z(V_\theta)} \mathbb{H}(u - z(V_r))e^{u^2}du, \tag{2.13}$$
$$p_{r,0} = \tau_{rp}\cdot\nu_{int,0}.$$

where $z(V) = \frac{V-\mu_0}{\sigma_0}$; an expression of the distance between the membrane potential and the mean input in units of the standard deviation of input. $\mathbb{H}$ is the Heaviside function. The normalisation condition, equation (2.11), gives us an expression for the *mean* firing rate, namely

$$\begin{aligned}\frac{1}{\nu_{int,0}} &= \tau_{rp} + 2\tau\int_{z(V_r)}^{z(V_\theta)} du\mathrm{e}^{u^2}\int_{-\infty}^{u} dv\mathrm{e}^{-v^2} \\ &= \tau_{rp} + \tau\sqrt{\pi}\int_{z(V_r)}^{z(V_\theta)} du\mathrm{e}^{u^2}(1+\mathrm{erf}(u)),\end{aligned} \tag{2.14}$$

where $\mathrm{erf}(u)$ refers to the error function

$$\mathrm{erf}(x) = \frac{2}{\sqrt{\pi}}\int_0^x \mathrm{e}^{-t^2}dt.$$

[3]This is a correction to the original paper [Brunel, 2000].

FIGURE 2.2: Dependence on external input in the inhibition-dominated Brunel model. The dependence of $\nu_{int,0}$ on $\nu = \frac{\nu_{ext}}{\nu_\theta}$ is approximately linear, as given by equation (2.15).
Model parameters: $J = 0.2$ mV, $C_E = 4000$, $\tau = 30$ ms, $\tau_{rp} = 2$ ms $V_\theta = 20$ mV, $V_r = 0$ mV.

An immediately obvious upper limit to the firing rate is the recovery period, or $\nu_{max} = 1/\tau_{rp}$.

We can use what we learnt in section 2.1 to define a dimensionless measure of the rate of external inputs. From equation (2.2) and equations (2.4) and (2.5), neglecting the terms representing recurrent inputs (i.e. setting $\mu_{int} = \sigma^2_{int} = 0$) we can solve the Langevin equation, to get $V(t) = V(0)\mathrm{e}^{-t/\tau} + C_E J \nu_{ext} \tau$. $V(0) = V_r = 0$ so we can see that the minimal rate and strength of external inputs for a neuron to (asymptotically) reach threshold is:

$$\nu_\theta := V_\theta / (C_E J \tau).$$

We can then measure external input in units of this threshold input, defining $\nu := \frac{\nu_{ext}}{\nu_\theta}$.

2.2.3 Firing rates

Values of $\nu_{int,0}$ which satisfy equation (2.14) can be found numerically. These results and analytic approximations by Brunel suggest the state space of the stable state can be roughly separated into regions in (ν, g)-space based on firing rates (see Figure 2.3):

1. $\nu > \mathbf{1}$, $\mathbf{g} < \gamma^{-\mathbf{1}}$: network is strongly driven with little recurrent inhibition, so firing rates are high, near saturation. In addition, considering networks with a large number of connections, we can expand equation (2.14) in powers of $1/C_E$. To first order precision, this

predicts

$$\nu_{int,0} \sim \tau_{rp}^{-1}\left[1 - \frac{V_\theta - V_r}{C_e J(1-g\gamma)}\right]$$

there is a smooth transition from this regime to the next ($g > \gamma^{-1}$) with increasing g. The slope of the transition, where $g \approx \gamma^{-1}$ becomes steeper with increasing C_E.

2. $\nu > \mathbf{1}$, $\mathbf{g} > \gamma^{-\mathbf{1}}$:In this case, inhibition dominates the network and, since all cells are being strongly driven, inhibitory cells don't generally need recursive input to become active, so sustained activity at low rates is possible. In the large C_E limit we can take advantage of the observation that consistent activity only occurs if the average recurrent activity, which is inhibitory, *just* offsets the excess external excitatory input. This condition is expressed as $\nu_{int,0}(1-g\gamma) = \nu_\theta - \nu_{ext}$. Hence the stable state rate should approximately follow

$$\nu_{int,0} = \frac{\nu_\theta - \nu_{ext}}{1-g\gamma}. \tag{2.15}$$

3. $\nu < \mathbf{1}$, $\mathbf{g} < \gamma^{-\mathbf{1}}$: In this region, two states are stable, a high frequency state and a quiescent state. We use the word *quiescent* in particular to stress that, in a true realisation of this system, the input to neurons is probabilistic so even if the mean input is sub-threshold, there is always *some* (possibly vanishingly small) probability that a neuron in the network may fire. The high activity state in this region is self-sustaining since the maximal firing rate ($\nu_{max} = 1/\tau_{rp} = 500.0$Hz) far exceeds the required threshold, even for small deficits in inhibition. Of course an intermediate fixed point must exist too, but is unstable. In figure 2.3a, we can see that the numerics find either the high-activity or the quiescent state, depending on the initial search condition.

4. $\nu \lesssim \mathbf{1}$, $\mathbf{g} > \gamma^{-\mathbf{1}}$: This region is of most biological interest. For most values of g, it is quiescent, but for a small region of $g \gtrsim 1/\gamma$ and/or $\nu \lesssim 0.75$, the global firing rate oscillates between quiescence and short bursts of activity. The periods of silence depend on how long it takes each neuron to reach threshold again depending only on external input and hence is principally dependent on $1/\tau$.

2.2.4 Inter spike intervals (ISIs)

So far we have considered regions of the parameter space of the Brunel model based on firing rates but an equally important characteristic statistic when trying to produce observed background

(A) (B)

FIGURE 2.3: Numerical characterisation of stationary states in the Brunel model. Solution to equation (2.14) plotted on a region of the $(\nu = \frac{\nu_{ext}}{\nu_\theta}, g)$ plane. These solutions are found numerically and so, in some regions, the initial search point effects which solution is found. Image (A) was calculated from an initial guess of $\nu_{int,0} = 5.0$. For image (B) searches began with an initial value of $\nu_{int,0} = 100$. For $\frac{\nu_{ext}}{\nu_\theta} > 1$ there is a clear divide between excitation dominated networks ($g < 4$), where rates are near saturation, and the much lower rates of of inhibition dominated networks ($g > 4$). Note that most of the $g > 4$, $\nu > 1$ region is *not* quiescent, but rather firing at rates far below saturation ($\nu_0 < 100$ Hz). Only a small number of "intermediate" states exist in a narrow band around $g \approx 4$, though these are of little biological interest. For $\nu < 1$, bi-stability appears for the region $g < 4$. Here, both high rates and the quiescent states are stable, the numerics finding either, depending on the initial guess value.

Network Parameters: $J = 0.2$ mV, $C_E = 4000$, $\tau \approx 31$ ms, $\tau_{rp} = 2$ ms $V_\theta = 20$ mV, $V_r = 0$ mV.

neural activity is the distribution of inter-spike intervals (ISIs). If each neuron is behaving like a Poisson process, we can expect the index of dispersion of *spike times* ($D := \frac{\sigma^2}{\mu}$) to be close to 1. Similarly, the time between events, or inter spike intervals should be exponentially distributed and hence the coefficient of variation of this quantity ($CV := \sigma/\mu$) should be approximately 1 in the regions of low firing activity.

The membrane depolarisation of an arbitrary neuron in the network is a random variable, obeying the Markov diffusion process described by a stochastic ODE: equation (1.3). The input term is equation (2.1). In the stable states solution (equation (2.13)), the average ISI is given by one-over the mean firing rate, $\frac{1}{\nu_{int,0}} = \mu_{0,ISI}$ (see equation (2.14)). The ISI is simply the escape time of the random variable $V(t)$ from the interval $(-\infty, V_\theta)$, given that the starting value was V_r. So the mean ISI is the first moment of the escape time about zero. By the theory laid out in appendix B.3, we can solve for higher moments of the ISIs. Note that the escape times, or ISIs are here considered functions of the initial/reset potential, V_r, so we let $x = V_r$.We refer to the definition of the infinitesimal generator of a diffusion process, or equation (B.5). For the Brunel model this is

$$\begin{aligned}
\alpha(x) &= \lim_{\Delta t \to 0^+} \frac{\mathrm{E}[X(t+\Delta t) - X(t) | X(t) = x]}{\Delta t} = \mathrm{E}\left[\dot{X}(t) | X(t) = x\right], \\
\alpha(x) &= \mathrm{E}[\tau^{-1}(-V(t) + \mu_0 + \sigma_0\sqrt{\tau}\eta_i(t)) | V(t) = x] \\
&= \tau^{-1}(-x + \mu_0),
\end{aligned}$$

since $\eta_i(t)$ is a white-noise process with zero mean. A similar calculation gives the infinitesimal variance:

$$\beta(x)^2 = \mathrm{Var}[\tau^{-1}(-V(t) + \mu_0 + \sigma_0\sqrt{\tau}\eta_i(t)) | V(t) = x] = \frac{\sigma_0^2}{\tau}.$$

The resultant infinitesimal generator for the process is:

$$(\mathcal{A}f)(x) = \frac{\sigma_0^2}{2\tau}\frac{d^2 f}{dx^2} + \tau^{-1}(\mu_0 - x)\frac{df}{dx}, \tag{2.16}$$

As pointed out by [Tuckwell, 1976], the higher order moments about zero can be found by solving equation (B.14). In our case, this is

$$\frac{\sigma_0^2}{2}\frac{d^2\mu_{n,ISI}}{dx^2} + (\mu_0 - x)\frac{d\mu_{n,ISI}}{dx} = -2\tau\mu_{n-1,ISI}(x)$$

FIGURE 2.4: Numerically calculated CV ISI values for the Brunel model in $(\frac{\nu_{ext}}{\nu_{thr}}, g)$ space. Variance in the interspike intervals is essentially zero in the excitation dominated regime. They jump quickly to ~ 0.8 once inhibition dominates and gradually approaches 1 with increasing inhibition, though is always slightly less than 1. These CV values are calculated from the $\nu_{int,0}$ values given in figure 2.3a

The second moment about zero, for $n = 2$ and $\mu_{1,ISI} = \frac{1}{\nu_{int,0}}(x)$ (see equation (2.14) for $V_r = x$) is

$$\mu_{2,ISI} = \mu_{1,ISI}^2 + 2\pi\tau^2 \int_{z(V_r)}^{z(V_\theta)} \mathrm{e}^{x^2} dx \int_{-\infty}^{x} \mathrm{e}^{y^2} (1 + \mathrm{erf}(y))^2 dy,$$

from which we can calculate the variance, since $\sigma_{ISI}^2 = \mu_{2,ISI} - \mu_{1,ISI}^2$. The square of the coefficient of variation, $(CV)^2 = \frac{\sigma_{ISI}^2}{\mu_{ISI}^2}$, is then

$$(CV)^2 = 2\tau^2\pi\nu_{int,0}^2 \int_{z(V_r)}^{z(V_\theta)} \mathrm{e}^{x^2} dx \int_{-\infty}^{x} e^{y^2} (1 + \mathrm{erf}(y))^2 dy \tag{2.17}$$

Given solutions for $\nu_{int,0}$ like those in figure 2.3, we can evaluate the CV value over a region of the (ν, g) plane.

Brunel used data like that in figure 2.4 to classify the dynamics as of this network as "regular/irregular" depending on whether the CV value of the inter-spike intervals is approximately 1 (as it should be for exponentially distributed spikes). Unsurprisingly, the CV value is approximately zero in the high activity state and approaches 1 quickly once inhibition dominates and the rates decrease. The CV only *approaches* 1 though, for most of the inhibition dominated regime $0.8 \lesssim \mathrm{CV} < 1$, so the dynamics do not appear to be truly Poissonian. Brunel used this result to classify regimes as regions of the (ν, g)-plane as Regular or Irregular.

In [Brunel, 2000], the author was principally interested in considering how solutions behaved in the (ν, g) plane. Brunel separates this plane into regions along the lines of regular/irregular firing and synchronous/asynchronous firing. Here, synchronous does not refer to true coupling between individual neurons. Rather, where the global activity displays some oscillatory behaviour, it is deemed *synchronous*, since "if the instantaneous firing rate ν_{int} varies in time, the spike trains will have some degree of synchrony". In contrast, he states spike trains "are uncorrelated only when global firing frequency ν_{int} is constant." The diffusive limit assumptions used in deriving the Fokker-Planck equation mean that the analytic predictions will not hold for networks where neurons experience significant correlations "beyond those induced by a common time-varying firing rate.". Before considering a specific extension to Brunel's parameter regime, we refer to figure 2.5 for an overview of the dynamic regimes this model produces. The key points are that no non-zero activity is stable for $\frac{\nu_{ext}}{\nu_\theta}$ values less than about 0.75 and that, even in regions dubbed "irregular", ISI CV values are less than 1.

Note that in [Brunel, 2000] considerable attention is given to showing where in the (ν, g) plane the mean global rate displays oscillatory dynamics. This is done by the usual means: using perturbation theory to find the Hopf bifurcation lines of the Fokker-Planck equation's steady state solution. Though interesting, this component of the analysis was not particularly useful for the analysis which follows here since one needs a closed (approximate) expression for the internal firing rate far from $\nu_{int,0} = 0$. Some progress has been made in this regard but, for purposes of brevity, the analysis has been omitted here.

2.3 Extension to Gewaltig Model

In [Gewaltig, 2013] it was shown by simulation that Brunel-like models could produce self-sustained activity in the absence of external inputs for long periods of time, provided the synaptic strengths J were relatively strong compared to threshold ($\frac{V_\theta}{J} \sim 3-7$). This formulation results in a trade-off: simulations would remain active for long periods for large synaptic inputs, but usually with firing rates of 30 Hz or more - much larger than generally observed in tissue. It was suggested that a Brunel network could become self-sustaining if only a small fraction of connections were strengthened significantly. In this section, I try to provide some novel analysis showing how this is possible. I will refer to networks of this form as Gewaltig models. The parameters for the Gewaltig model are identical to those above, except that a random fraction f of inputs to each neuron are strengthened by a factor α. Returning briefly to the spike train

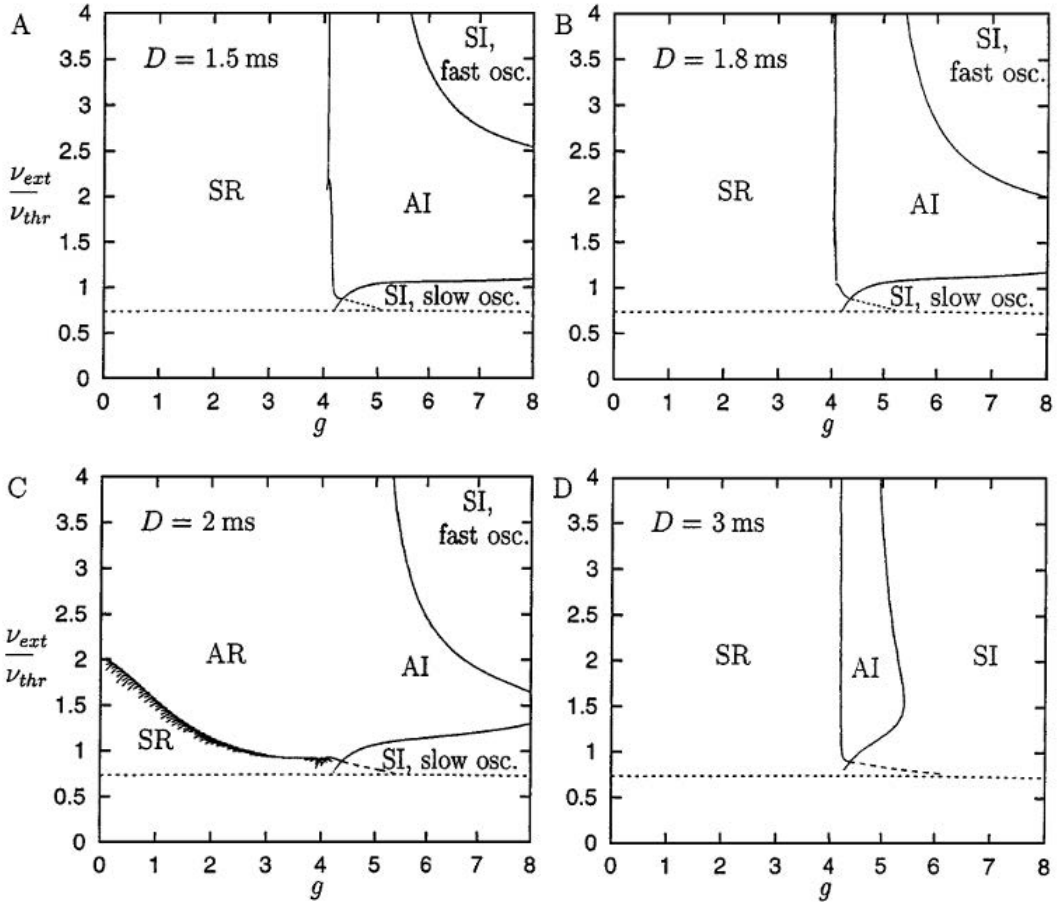

FIGURE 2.5: SR stands for *synchronous regular*, AI for *asynchronous irregular* etc. **A:** The "canonical" case. For adequately driven, excitatory dominated states ($g < 4$, $\frac{\nu_{ext}}{\nu_\theta} > 0.75$), neurons fire synchronously and regularly near saturation. Once inhibition dominates, activity becomes asynchronous: the global rate is approximately constant and individual neurons fire due to fluctuations from a sub-threshold mean: hence spike times are irregular. For large ν_{ext} and large g, a Hopf bifurcation occurs to a region of fast global oscillation, with synchronous irregular firing. For $g > 4$ and $\frac{\nu_{ext}}{\nu_\theta} \sim 1$, the AI state again undergoes a Hopf bifurcation to slow global oscillation with irregular individual neuron firing. **B-D** show how these bifurcation lines shift for differing delay values. **C:** for $D = \tau_{rp} = 2$ms, a large portion of the Synchronous Regular region becomes Asynchronous. **D:** for $D = 3$ neurons can recover between consecutive spikes from the same afferent neuron, so the network operates on somewhat of a "time grid" defined by the delay, hence acitivity is synchronous. For the inhibitory dominated regime, though, a neuron may be receiving enough inhibition not to spike, so spike times are not necessarily regular. The dotted line indicated where the stable quiescent state destabalises.

Network Parameters: $J = 0.2$ mV, $C_E = 4000$, $\tau \approx 31$ ms, $\tau_{rp} = 2$ ms $V_\theta = 20$ mV, $V_r = 0$ mV. Taken from [Brunel, 2000].

formulation of equation (C.1), the input to each cell becomes:

$$RI_i(t) = \tau\Sigma_j^{C_n} J_{ij}\Sigma_k \delta(t - t_j^k - D) + \tau\Sigma_j^{C_\alpha} \alpha J_{ij}\Sigma_k \delta(t - t_j^k - D), \tag{2.18}$$

where C_n and C_α are integers satisfying $C_n + C_\alpha = C$ and $C_\alpha/C_n = f$.

As a crude first approach, let us assume we can still represent this input as a Gaussian process, though with an appropriate adjustment of the mean and variance. Using the subscript α to denote contributions from this class of stronger connections, the input from these connections to an arbitrary neuron's soma can be written as

$$RI_{i,\alpha}(t) = \mu_\alpha(t) + \sigma_\alpha(t)\eta_i(t),$$

where

$$\begin{aligned}\mu_\alpha(t) =& fC_E\alpha J(1 - \gamma g)\nu(t - D)\tau = \mu_{int}\alpha f \\ \sigma_\alpha^2(t) =& fC_E(\alpha J)^2(1 + \gamma g^2)\nu(t - D)\tau = \sigma_{int}^2\alpha^2 f\end{aligned} \tag{2.19}$$

and μ_{int} and σ_{int} are those values of the conventional Brunel model (equation (2.4) equation (2.5)). We can thus think of our system as now consisting of an *extremely* sparse, strongly connected network embedded in a sparse, weakly connected network. Summing the inputs from both networks to neuron i we obtain expressions for the mean and variance of the total input to each neuron,

$$\begin{aligned}\mu(t) =& \mu_{ext}(t) + \mu_{int}(t)(1 + (\alpha - 1)f), \\ \sigma^2(t) =& \sigma_{ext}^2 + \sigma_{int}^2(t)(1 + (\alpha^2 - 1)f).\end{aligned} \tag{2.20}$$

Looking at these expressions, we can already see that, for values of $f = 0.01, \alpha = 20$, the mean input to each neuron is only mildly effected, but the change in variance of the internal input grows nearly five-fold. This is important because, as shown in [Vreeswijk and Sompolinsky, 1996], Poissonian statistics of the spike times can be the result of internal network dynamics even if the external input is constant ($\sigma_{ext} = 0$) and, as explained in [Gerstner and Kistler, 2002], an individual neuron displaying Poissonian spiking statistics is associated with noisy input with sub-threshold mean (see section 2.1).

2.3.1 Fixed-point analysis

For ease of discussion, let us now re-write equation (2.14) as

$$G(\nu_{int}, \nu, g, f, \alpha) = \left(\tau_{rp} + \tau\sqrt{\pi} \int_{z(V_r)}^{z(V_\theta)} du e^{u^2} (1 + \mathrm{erf}(u)) \right)^{-1} - \nu_{int}, \tag{2.21}$$

where dependence on $\nu = \frac{\nu_{ext}}{\nu_{thr}}, f, g, \alpha$ lies in the function $z(V) = \frac{V - \mu(\nu_{int}, \nu)}{\sigma(\nu_{int}, \nu)}$, with equations (2.4), (2.5) and (2.19) and equation (2.20). G is then a function of dimensionless parameters and again, mean firing rates are found by solving for roots of equation (2.21) in ν_{int}. Roots of G for $\nu \neq 0, f = 0$ correspond to fixed points in the Brunel model while for $\nu = 0, f \neq 0$ we have the Gewaltig model.

We let $\nu = 0$ and consider, without loss of generality, the $V_r = 0$ case. Then the upper and lower limits of the integral in G can be written $z_\theta = \frac{V_\theta - \mu_{int}}{\sigma_{int}} = \frac{V_\theta - \mu_G \nu_{int}}{\sigma_G \sqrt{\nu_{int}}}$ and $z_r = \frac{-\mu_{int}}{\sigma_{int}} = \frac{-\mu_G \sqrt{\nu int}}{\sigma_G}$ respectively, where

$$\mu_G := C_e J \tau (1 - g\gamma)(1 - (\alpha - 1)f)),$$
$$\sigma_G^2 := C_e J^2 \tau (1 + g^2\gamma)(1 + (\alpha^2 - 1)f)).$$

In the limit $\nu_{int}^+ \to 0$, $z_\theta \to \infty$ while $z_r \to 0$ and, since the integrand is positive everywhere, the integral becomes infinite, so G becomes zero. Note that this would *not* be true for the $\nu \neq 0$ (Brunel) case, wherein the integral limits would remain finite and hence G would be small but non-zero.

As ν_{int} gradually increases from zero, initially $G \sim \nu_{int}$ but eventually the integral shrinks rapidly and the term $\left(\tau_{rp} + \tau\sqrt{\pi} \int_{z(V_r)}^{z(V_\theta)} du e^{u^2} (1 + \mathrm{erf}(u)) \right)$ becomes of comparative size to $1/\nu_{int}$. The integrand is a rapidly growing function and so the integral shrinks considerably when the distance between the integral limits shrinks rapidly. The lower limit of integration follows $z_r \propto \sqrt{\nu_{int}}$ but for small ν_{int}, the upper limit is dominated by the term $z_\theta \sim \frac{V_\theta}{\sigma_G \sqrt{\nu_{int}}}$. So a rough value for the point at which the integral becomes small enough for G to first re-intersect the axis occurs when the terms in z_θ begin to balance each other out. This can be found by solving

$$\frac{dz_\theta}{d\nu_{int}} = -1, \tag{2.22}$$
$$\Rightarrow \nu_- (2\sigma_{int}\sqrt{\nu_-} - \mu_{int}) - V_\theta \approx 0. \tag{2.23}$$

We use ν_- to denote this lower, unstable fixed point.

In the limit $\nu_{int} \to \infty$, we can see that $z_r \to z_\theta \to \frac{-\mu_{int}}{\sigma_{int}}\sqrt{\nu_{int}}$ and hence the integral closes off, becoming zero. The first term of G then becomes τ_{rp}^{-1} and hence the ν_{int} value once again dominates and G becomes negative. Hence we know there must be a third, upper root, denoted ν_0. This root is the one we are most interested in as it represents self-sustained non-zero firing rates. Since the limits approach each other, we can rewrite the condition $G = 0$ as

$$\tau_{rp} + \tau\sqrt{\pi}\int_{\frac{\mu_{int}}{\sigma_{int}}x}^{\frac{\mu_{int}}{\sigma_{int}}x+\epsilon(x)} \mathrm{e}^{u^2}(1+\mathrm{Erf}(u))du - 1/x^2 = 0, \tag{2.24}$$

where $x = \sqrt{\nu_{int}}$ and $\epsilon(x) = \frac{V_\theta}{x\sigma_{int}}$. Hence ϵ shrinks with growing ν_{int} and we can expand the integral around $\epsilon = 0$. Letting $a := \frac{-\mu_{int}}{\sigma_{int}}x$, this gives us the expressions (to order $\mathcal{O}(\epsilon^3(x))$

$$\begin{aligned}\tau_{rp} + \tau\sqrt{\pi}\Bigg(&e^{a^2}(1+\mathrm{Erf}(a))x + (\frac{1}{\sqrt{\pi}} + ae^{a^2}(1+\mathrm{Erf}(a)))x^2 \\ &+\frac{1}{3}\left(\frac{2a}{\sqrt{\pi}} + (1+2a^2)e^{a^2}(1+\mathrm{Erf}(a))\right)x^3\Bigg) - 1/x^2 = 0\end{aligned} \tag{2.25}$$

Numerical solutions to this expression give a fairly accurate approximation to the upper root but is of little use for perturbation analysis of the Fokker-Plank equation (see [Brunel, 2000]).

Figure 2.6 shows a comparison of several realisations systems: the Brunel model, Gewaltig model and the Gewaltig model with external input. Most importantly, it shows that the true Gewaltig model ($\nu = 0$, figure 2.6a) does not have a *globally* stable non-zero fixed point, but always has a stable fixed point at $\nu_{int} = 0$[4]. Thus the next fixed point from the origin is expectedly *unstable* while the third, upper fixed point is again (locally) stable. If we consider external input ν too, we can see that the appearance of bi-stability can only occur when $\nu = 0$. If $\nu > 0$, increasing f simply has the effect of shifting the single root up. Thus we have that the system experiences a *codimension-2 imperfect saddle-node bifurcation* [Strogatz, 1994]. The strength of external input, ν, is known as an imperfection parameter. For $\nu > 0$, only one fixed point exists and is globally stable but for $\nu = 0$ there is the possibility of a saddle-node bifurcation with increasing f to produce the fixed points ν_- (unstable) and ν_+ (stable). Note that throughout this text we will denote the upper fixed point as $\nu_{int,0}$ or sometimes just ν_0.

[4]To be precise, equation (2.14) (and hence the derived equation (2.21)) is ill-defined when both $\nu_{ext} = 0$ and $\nu_0 = 0$. It is obvious, though, that the system, with no external input, cannot ever fire for $\nu_{int}(0) = 0$. For numerical root finding purposes, this is not a problem, as the limit $\lim_{\nu_{int}\to 0} G(\nu_{int}, \nu = 0) = 0$.

(A) (B)

FIGURE 2.6: Co-dimension 2 imperfect saddle-node bifurcation. Solid dots indicate stable fixed points. The f values for solid lines apply to both plots. Dashed lines indicate the Brunel model ($f = 0$). **(A)** $\nu = 0$. The open circle indicates the unstable fixed point for the $f = 0.006$ case. All other unstable fixed points have been omitted for clarity. At $f = 0$, only the zero rate state is stable. As f increases two new solutions appear when $f \lesssim 0.006$. The zero rate state remains stable in all cases (see footnote 4). **(B)** $\nu > 0$. The origin is **only stable** for the blue line ($\nu = 0.5$). Only one stable solution exists for each system. All solid line are for $\nu = 0.5$ and with f values as indicated (Gewaltig model with input). Note that for ν below threshold ($\nu < 1$) there is not enough external input to bring the Brunel model ($f = 0$) out of the quiescent state. For $f > 0$, increasing f simply amplifies the mean and the variance in the recurrent input, increasing the firing rate above zero. The key point is that the saddle-node bifurcation to bi-stability can only occur if $\nu = 0$ and that the system has only one stable state if $\nu > 0$.

Network Parameters: $J = 0.2$ mV, C_E=4000, $g = 5$, $V_\theta = 20$ mV, $\tau_{rp} = 2$ ms, $\tau = 30$ ms, $\gamma = 0.25$, $\alpha = 30$.

Figure 2.7a shows the sigmoid nature of the root ν_0 in a reasonable region of the (f, g) plane, while figure 2.7b shows how rates decrease with growing g.

2.3.2 Firing rates and CV values

Compare the red line in figure 2.6a (Gewaltig) to the blue-dashed line in figure 2.6b (Brunel). We can see that, to produce similar low firing rates, this Gewaltig model ($\alpha = 30$) needs only a very small fraction of strengthened connections ($f = 0.006$) but that the upper stable fixed point and intermediate unstable fixed point lie quite close together. If even a small amount of external input is added (the red line in figure 2.6b) the value of the stable-state rate increases significantly. Hence we have that firing rates predicted by the Gewaltig model are significantly higher than those predicted for the Brunel model with similar parameters. Of course, with "fine tuning", the Gewaltig model can have ν_0 values less than 10 Hz but, as explained in the following chapter this results in a vary small basin of attraction for the upper fixed point.

Equation (2.17) allows us to calculate CV values for the Gewaltig model too. These are plotted for the canonical parameter set in figure 2.8. The first thing to note is that the CV values predicted for the inhibition-dominated region are significantly more than 1, unlike in the Brunel case. This suggests that the inter-spike intervals of individual neurons are distributed very much exponentially. This is in agreement with what we would expect from the results of [Vreeswijk and Sompolinsky, 1996], where a sparse but strongly connected network displayed highly chaotic dynamics. High ISI CVs were also observed by the author of [Gewaltig, 2013] in the simulation data. In that paper it was noted that ISI data could be separated into multiple sets, each well-fitted by a Poisson process of a different rate. The global distribution of ISIs is then simply the convolution of the various exponential distributions with different rates. These widely distributed ISI values point to the bursting dynamics of neurons in the network. What this means is that, if we observed an individual neuron, it would appear to switch between periods of relatively large ISIs and short "bursts" of rapid firing. In all, these results agree with the intuition obtained from section 2.1 and equation (2.20): the significant increase in the input variance leads to larger fluctuations being experienced by each neuron, even though the mean input remains essentially balanced. This results in a wider *spread* of the membrane distributions as they leave the resting state (see figure 2.1) and hence a wider distribution of ISIs.

(A)

(B)

FIGURE 2.7: (A) shows the sigmoid-like shape of the locally stable fixed point $\nu_{int,0}$ in the (f, g) plane. (B) shows data from the $g > \gamma^{-1} = 4$ region of (A) plotted on a logarithmic scale. Note that for $g \sim 5$, rates of $5 < \nu_{int,0} < 10$ can be obtained for very small fractions of strengthened connections ($f = 0.005$). When the system is strongly over-damped, reasonably low rates become realisable for $f \geq 0.01$.

Network Parameters: $J = 0.2$ mV, $C_E = 4000$, $\tau = 30$ ms, $\tau_{rp} = 2$ ms $V_\theta = 20$ mV, $V_r = 0$mV.

FIGURE 2.8: ISI CV values of the Gewaltig Model. CV values are zero over the excitation dominated region, as neurons are firing rapidly and repeatedly here. The CV value "spikes" in the transition region, where $g \simeq \gamma^{-1} = 4$, though rates are still high. This is because, in this region, the population rate fluctuates enormously. CV values remain significantly larger than 1 for $g > 4$. This supports the observations of [Gewaltig, 2013] that, in simulations, neurons in the display bursting spiking patterns (see text). Note the increase in CV with increasing f for fixed g.

Parameters:$J = 0.2$mV, $C_E = 4000$, $\tau = 30$ms, $\tau_{rp} = 2$ms $V_\theta = 20$mV, $V_r = 0$mV.

Chapter 3

Comparison to Simulations and Limitations

The analysis described in the preceding chapter allows us to predict whether we should find self-sustaining dynamics in systems of sparsely connected networks of integrate and fire neurons. As a first step in testing the validity of this analysis, we used NEST software to simulate realisations of these models for different parameter values. See appendix E for descriptions of the simulation details. In this chapter, we will discuss the results of these simulations and compare them to the predictions of the analysis.

3.1 Rates and Inter Spike Intervals

The simple adjustment of the Brunel model to the Gewaltig model (as proposed in section 2.3) has allowed us to capture two essential aspects evident in the simulation results of [Gewaltig, 2013]: the bifurcation to the existence of self-sustaining states and the dramatic increase in variability of spike rates, pushing inter-spike interval CVs well above unity for the inhibition dominated case. It also allows us to roughly estimate the survival times of network realisations, as discussed below in section 3.2.

Figure 3.1 shows the some analytically predicted rates compared to those of simulations. As f increases, the analysis increasingly underestimates the rates found in simulation. We can understand why this is the case due to a break-down of the diffusion approximation with increasing f. Our analytic formulation of the Gewaltig model relies on the validity of the Fokker-Planck

FIGURE 3.1: The blue line indicates the analytically predicted firing rates of a Gewaltig system for differing f values. The lower, red line, shows the value of ν_θ (equation (3.1)) for the same system. This is an estimate of the "boundary" of the basin of attraction for the fixed point ν_0. The error bars span two standard deviations of the firing rate, namely $2\sqrt{\nu_0}$. The dots denote the mean global firing rate from multiple, independent simulations for that f value. No values are given for $f = 0.005$ because no networks remained self-sustaining for this case. For the $f = 0.01$ case, several simulations survived for less than 50 ms (see figure 3.2) and so the total sample size of spikes were very small. Calculated global averaged rates for these realisations were low and these are the dots which appear below the red line. See the text for a discussion of the differences in rates observed and those predicted.

Network parameters: $C_E = 10^3$, $\epsilon = \frac{C_E}{N_E} = \frac{C_I}{N_I} = 0.1$, $\gamma = \frac{C_I}{C_E} = \frac{N_I}{N_E} = 0.25$, $g = 5$, $\tau_{rp} = 2$ ms, $\tau = 30$ ms, $J = 0.1$ mV, $\alpha = 40$.

description of the system. This equation is valid in the diffusive approximation limit (appendix C.2) where the membrane potentials can be described by a diffusion process because the global activity is well approximated by a mean rate with normally distributed fluctuations and individual inputs are small. But for large connection strengths, individual inputs are large, causing "jumps" in the membrane potential. These diffusive limit approximation no longer holds. This is why the work in [Gewaltig, 2013] and [Kriener et al., 2014] is done by simulation. In the "strong connection" limit, the inputs to individual neurons are better described by a *jump* process (or random walk). For the Gewaltig model, as f simulations should they become increasingly better approximated by diffusion processes with significant jump components - or *jump-diffusion processes* rather than simple diffusion processes. The full general form of the stochastic integral equation which describes a Markov process with diffusion and jump components is given in appendix B, equation (B.9).

So the natural improvement to our analytic model would be treat the membrane potentials of

f	0.01	0.015	0.02
Analysis	1.33114	1.57951	1.76054
Simulation	0.511781 ± 0.172527	1.99828 ± 0.361008	2.68477 ± 0.302494

TABLE 3.1: Comparison of the coefficients of variation (CVs) for simulations and analysis of the "canonical" Gewaltig model during the self-sustaining states. Mean and standard deviation of CV is given for $n = 10$ realisations of each simulation. Both analysis and simulation capture a key feature: that self-sustaining states are highly irregular, with $CVs > 1$. For $f = 0.01$ the majority of simulations have very short survival times, so there are very few inter spike intervals to gather. This data is somewhat less reliable and could be improved by running a much larger number of simulations. With increasing f, simulations record larger CVs than predicted by the analysis. This is most likely due to the increasing inaccuracy of the diffusion approximation in accounting for the fraction f of strengthened connections.Simulation parameters: $C_E = 10^3$, $\epsilon = \frac{C_E}{N_E} = \frac{C_I}{N_I} = 0.1$, $\gamma = \frac{C_I}{C_E} = \frac{N_I}{N_E} = 0.25$, $g = 5$, $\tau_{rp} = 2$ ms, $\tau = 30$ ms, $J = 0.1$ mV, $\alpha = 40$.

neurons in the Gewaltig model as jump-diffusion processes with the jump component given by a compound Poisson processes designed to approximate the inputs from the fC_E strengthened connections. We then have a natural extension to the Fokker-Planck equation, similar to that described in [Inordunatum, 2013], namely

$$\tau \frac{\partial P}{\partial t} = \frac{\sigma(t)}{2} \frac{\partial^2 P}{\partial V^2} + \frac{\partial}{\partial V}[(V - \mu(t))P] - \lambda P(t, V) + \lambda \int_{-\infty}^{\infty} Q(S)P(t, V - S),$$

where $\lambda = f\nu(t)$ is the mean rate of the jump component and $Q(S)$ is the distribution of jump sizes. When solving for the stationary state value of $P_0(V)$, we will be solving an integro-differential equation or, at best, difference-differential equation in $P_0(V)$. I am currently undertaking to analyse this formalism to see if we can improve on the predicted values of firing rates.

For now, we can gain some insight by noting that this jump term will *increase* the variance in the input to individual neurons, more so than the simple diffusion introduced in equation (2.20). We would expect this enlarged variance in input to push firing rates up, as well as increase the ISI CV of simulations above those predicted by the analysis. This inclination is supported by the data in table 3.1 where simulations measure significantly larger CV values than predicted by the analysis. See chapter 4 and [Kriener et al., 2014] for further support of this argument.

3.2 Survivability of stable-states

In the analysis of chapter 2, we are studying a deterministic model for the expected, or mean, values of firing rates. In simulations of the networks, the random connectivity of the independent realisations, as well as the random nature of the initial input to the network introduce noise

to the system. As mentioned in chapter 1, and supported by simulation and our earlier CV analysis, we expect the neurons to fire like Poisson processes and, hence, the global rate is also a Poisson process. So we do not expect a (finite network size) simulation to *rigidly* maintain a firing rate of $\nu_{int,0}$, rather we expect the firing rate to *fluctuate* around this value. For the Brunel network, this is not a problem as the mean-field analysis predicts only the single mean rate is stable, so for small fluctuations, the mean firing rate always returns to $\nu_{int,0}$. But for the Gewaltig network there is always some non-zero chance that the network *could* fluctuate enough from the mean ($\nu_{int,0}$) such as to leave the attractor basin[1]. Since there is only one other attractor (the silent state), the network would then return to the silent state. A good question, then, is how likely this is to happen?

Below we develop a simple means of predicting the survival time of realisations of Gewaltig networks, giving us an idea of how stable the model is for different parameters. It makes sense to consider "survival time" because, if fluctuations are independent and of arbitrary size (distributed around the mean: $\nu_{int,0}$) then, given long enough, the probability of a "large enough" fluctuation occurring approaches 1. Note that, after this work was done, the author became aware of a very similar approach used in [Kriener et al., 2014]. We use the diffusive limit approximation from appendix C.1. We assume that the network is unlikely to maintain its activity if the mean recurrent input drops below that required to reach threshold in the Stein model, namely[2]

$$\nu_0(t) < \frac{V_\theta}{C_E J \tau (1 + (\alpha - 1) f)} = \nu_\theta.$$

Note that here we write $\nu_0(t)$ to denote the *average* firing rate across the network of a simulation which is no longer receiving external input. As we're assuming fluctuations to be normally distributed around the mean rate of $\nu_{int,0}$ (and statistically independent), the probability that the global firing rate drops that low is given by

$$Pr\left\{\nu_0(t) < \nu_\theta\right\} = \frac{1}{2} - \frac{2}{\sqrt{\pi}} \int_0^{\frac{\nu_\theta - \nu_0}{\sqrt{2\nu_0}}} e^{-u^2} du \tag{3.1}$$

We can see that although small values of f predict low rates, they also predict increased likelihood of network failure since the mean rate is well within a standard deviation of the threshold.

[1] Note that, in the infinite network limit, these fluctuations are negligible, hence we speak of the expected value fixed point, $\nu_{int,0}$, as being "stable" in the earlier analysis.

[2] Note that we do not say $\nu(t)$ becomes unstable if it fluctuates below ν_-. Equation (2.21) is not a *dynamic* equation governing $\nu(t)$, rather it governs the dynamics of $E[\nu(t)]$ in the infinite network limit. Hence we use a normally distributed random process to approximate the global mean, $\nu(t)$ fluctatues during a simulation.

FIGURE 3.2: Lines denote the value of equation (3.2) for three f values, evaluated for the ν_0 values predicted by analytics. Dots denote the final spike times of simulations of that system. The dots are placed on the lines to improve readability, as that is the calculated probability of a simulation surviving that long. The majority of simulations for $f = 0.02$ survive almost 10 times as long as simulations for $f = 0.01$. The distribution of survival rates indicates that decay to the ground state is not a simple effect of dampening due to feed-back being predominantly inhibitory. Note that in no way does the value of f effect the ratio of excitation to inhibition and that, in all cases, simulations were driven with the same initial Poissonian activity for a duration of 200 ms.

Simulation parameters: $C_E = 10^3$, $\epsilon = \frac{C_E}{N_E} = \frac{C_I}{N_I} = 0.1$, $\gamma = \frac{C_I}{C_E} = \frac{N_I}{N_E} = 0.25$, $g = 5$, $\tau_{rp} = 2$ ms, $\tau = 30$ ms, $J = 0.1$ mV, $\alpha = 40$.

Since the diffusive approximation applies in the $N \to \infty$ limit, our calculation should become increasingly accurate for larger network sizes.

We can take this analysis one step further and attempt to anticipate how long a network for which our mean-rate analysis *predicts* stability should actually survive. We note that the firing rate at time t depends principally on the rate at time $t - D$. Suppose we can then treat fluctuations in the global firing rate over periods of D as mutually independent events. The probability of a simulation surviving from $t = 0$ to at least time t_{end} is then the probability of it surviving all intervals of length D up until t_{end}. This is given by

$$Pr\left\{\nu_{int}(t_{end}) > 0\right\} = \frac{1}{2} + \frac{2}{\sqrt{\pi}} \int_0^{\frac{\nu_\theta - \nu_0}{\sqrt{2\nu_0}}} e^{-u^2} du. \tag{3.2}$$

Figure 3.2 shows the predicted survival rate of the Gewaltig model for various f values. For comparison, it also shows the survival time of multiple small-scale simulations of the system. There is obviously a large variation between the survival times of individual simulations, for

example, simulations with $f = 0.02$ survived for between less than a second to more than 10 seconds. Still, there is a strong dependence on f in survival times, with most networks with $f = 0.02$ surviving more than 100 times as long as simulations with $f = 0.01$.

At a late stage of preparation of this thesis, the author became aware of the work in [Kriener et al., 2014] which is an extension of the work in [Gewaltig, 2013]. Kriener et al. focus on the strong connection case. They point out the saddle-node bifurcation to self-sustained activity as a result of increasing synaptic strength, but do not note that, if we consider the external input too, we have the co-dimension two bifurcation mentioned in section 2.3.1. Since their work is predominantly numerical, they make use of some of the detailed connectivity data in [Song et al., 2005] and argue that this supports the existence of self-sustainability in cortex. They monitor the membrane potential of a neuron in the network with "infinite threshold" which shows how fluctuations in the population rate can push the input of an individual neuron well above threshold for relatively long periods of time (several times the reseting period τ_{rp}). It is during these periods that the neurons are observed to be bursting. They provide similar calculations to predict the survival time of simulations to those given above. They too assume (and support with simulation) that network rate fluctuations are normally distributed and state that "If the basin of attraction is smaller than the characteristic fluctuation size, the system can escape the attractor and run into the trivial attractor at zero rate." They obtain exponential increases in survival time (by simulation) with increasing connectivity J. In their discussion, they point out that their analysis (using the Abeles two-state model [Abeles, 1982]) also under-predicts firing rates seen in simulations. They state that part of the fault is the self-consistency argument of the analysis: assuming the network neurons are behaving like Poisson processes, it seeks to re-produce a process with variance *greater* than that of a Poisson process. Simulations show that, in the self-sustaining state, neurons show greater variation than that expected for a Poisson process, which must be incorporated into the analysis.

Chapter 4

Conclusions

Networks consisting of simple neuron models, such as the integrate-and-fire neuron, do not capture the detail and parametric complexity of real biological systems. A broad, generally open question in all of theoretical biology (and modelling at large) is *how much of what we observe is necessary for function? Or is it simply the complex machinery evolved by nature to produce a beneficial function?* Spiking-network models help us to address this by seeing how much of the dynamics and computation we observe in biology can reproduced without using structures with as much complexity as real biological neurons (i.e. ion channels, dendritic effects, etc.). They help us to develop our intuition for the more complex biological processes occurring at the network level. These "toy models" allow us to relate observed dynamic processes to theoretical computational processes which helps to guide future, more costly experiments. In this thesis, the underlying mathematical principles are emphasised and with good reason: if we hope to develop more sophisticated models which better capture the dynamics and higher-order statistics observed in experiments, young theoretical neuroscientists will need to be increasingly adept at mathematical analysis [Gerstner et al., 2012, Laing, 2014, Mitry et al., 2013].

The key points to take away from this thesis are:

- Theoretical networks of sparse and randomly connected integrate-and-fire neurons can maintain locally stable self-sustained activity of the mean network firing rate. We can think of this as coming about via a codimension-2 imperfect saddle-node bifurcation in the (ν_{ext}, f) plane, where ν_{ext} is the external input (imperfection parameter) to the system and f the fraction of strengthened connections.

- All noise in the Gewaltig model is introduced by randomised external input and randomised connectivity. Thus although the expected value of the global firing rate is locally stable, for any individual realisation of the system there is a probability that the trajectory of the system will escape the basin of attraction for the upper fixed point and decay to the silent state. Under the diffusive limit approximation and the arguments in chapter 3 we expect networks with a larger strengthened fraction (larger f) to survive longer and this is indeed what we find. These results are in agreement with the similar analysis given in [Kriener et al., 2014]. Any realisation of such a network will become silent in finite time.

- Individual neurons switching between bursting/low-rate firing in these models does not require the inclusion of constant external noise or cellular bi-stability. It is be observed as a result of network dynamics and results in large variances of inter-spike intervals, something widely observed in experiment.

If we interpret a Gewaltig network as a sub-network of a larger tissue, then the self-sustained states shown have persistent activation qualities similar to those observed in delay response experiments [Compte et al., 2000, Compte et al., 2003]. This mechanism for working memory was developed in [Amit and Brunel, 1997] but, as pointed out in [Barbieri and Brunel, 2008], the ISI statistics in the delay activity states of that model are far from random (CV$<<1$). The Gewaltig model discussed here overcomes this problem, with CV values of the order of $1.7-2.6$ (in simulation) for the self-sustained activity state ($f = 0.015-2$). These are extremely cautionary conclusions and more work must be done on simulating and analysing this model in the sub-network context.

From the models and and associated papers discussed in this thesis, the broad conclusion taking shape is that the dynamics of cortical substructures can be captured as a combination of external driving and those of self-sustained activity, which is possible due to the presence of a smaller number of significantly stronger connections [Kriener et al., 2014]. The connectivity data we have for these brain regions allows for both to be present and, while one easily allows for the background rates observed, the other captures the high variability of inter-spike intervals and the burstiness of individual neurons. There is no doubt that much detail could be added to these models in terms of connectivity[1] which may help them better fit a wider array of experimental

[1] A notable exception to this may be accounting for the strong connectivity clustering observed in [Song et al., 2005]. This would introduce significant correlations to neuron spike trains which makes analysis more difficult but is presumably essential for information processing.

data but I do not feel this will bring significant insight to our understanding of neural dynamics or neural computation. In analytic studies we often differentiate between "weakly connected" and "strongly connected" models, but we know that, in biology, most networks have long-tailed connectivity distributions. Similarly, I feel that arguments that these models require require "fine tuning" to produce reasonable spike statistics are invalid, since the analyses only consider the means and variances or the resultant input [Renart et al., 2007, Vreeswijk and Sompolinsky, 1998, Vreeswijk and Sompolinsky, 1996]. There is still work to be done in assimilating this line of research with others. For example, the work of [Sussillo et al., 2007] proposes an alternative means for stabilizing intermediate firing rates, namely by the mechanism of short-term synaptic plasticity. Short-term synaptic plasticity is a widely accepted phenomenon [Tsodyks et al., 1998] and there is currently much work underway to acceptably include it into spiking network models.

The overall conclusion of the collective literature on networks of simple spiking neurons is that this framework is steadily growing to capture the dynamics commonly observed in cortical tissue experiments. This provides increasing support for the argument that sophisticated neuron-level dynamics (or sub-neuron dynamics, for ion currents etc.) are probably not fundamental to capturing the network level dynamics observed in experiments. In particular it suggests that we may be able to understand and reproduce the information processing which occurs in neural tissue without complex individual neuron structures. This is by no means conclusive but, if we combine this trend with the increasingly accepted idea that neural computation occurs predominantly due to activity at the micro-network scale, we begin to see a picture in which brain-like information processing can be achieved with systems of vastly less complexity than that observed in biology.

The approach taken in this thesis is lacking in some key regards. Firstly, all of the models discussed are constructive, trying to reproduce observed activity statistics from "first principles". This is the natural approach of biological modelling but the field has reached the point where the approach needs changing. We should see observed firing rates and inter-spike-intervals as the *result* of some underlying information processing procedure. They are benchmarks against which to check whether our models for information processing are in agreement with biology [Ostojic, 2014]. This is the direction in which computational neuroscience research is going. Important new themes of research include the consideration of correlations in global network activity [Ostojic et al., 2009, Tchumatchenko et al., 2010, Grytskyy et al., 2013] and focus on

the process of coupling and synchronization between individual neurons [Knoblauch et al., 2012] via mechanisms like spike timing dependant plasticity (STDP) [Markram et al., 2012].

The second point is similar: we should not see the connectivity data as an observed, necessary parameter to achieve the network dynamics we want. Rather we should expect observed distributions to be the result of the dynamic processes of synaptic plasticity and/or learning. Multiple branches of research are already pursuing this [Levina et al., 2007, Torres and Kappen, 2013] with some fascinating results. An intriguing idea is that neural systems perform computations on time series of spikes and that this process is optimised if the system dynamics are on "the edge of chaos" [Bertschinger and Natschläger, 2004]. I feel this is the next major hurdle in the study of spiking neural networks: understanding how the interplay between network spike dynamics and network plasticity dynamics result in information processing.

Development of detailed spiking neural networks and efficient means of simulating them can provide us with several tools for neuroscience. The first is a means to quickly gather insight into how observed connectivity data (or shifts in connectivity data) should effect network level dynamics. The other is a platform for the design and testing of information processing models, based on spikes. The principle mathematical challenges posed by the field are:

- the design and analysis of simple neural models and synaptic dynamics models which sufficiently capture those observed in the lab (essentially dealing with complexity),
- bifurcation analysis in the (often large) parameter space of the networks,
- analysing the coupled dynamics of networks and connections,
- designing and analysing means by which information can be encoded by spiking systems and understanding how algorithms would be executed to process this information.

Appendix A

Measure Theory to Stochastic Calculus

The principle mathematical techniques used in the analysis of spiking neural network models are probability theory, the theory of stochastic processes and the theory of dynamical systems. Although the analysis presented in this thesis does not draw on the deep results of these fields, for purposes of rigour, I give several appendices outlining important definitions and key results. I will assume the reader has some intuitive understanding of probability theory. Most important theorems will simply be stated and proofs generally omitted but referenced.

Measure theory studies the abstraction of the concept of "measuring" the size of subsets of a set. The "size" is given by the values taken by a function when evaluated on a subset. This function is called a measure. The purpose of this section is to familiarise the reader with the underlying measure theoretic concepts and basic stochastic calculus as this will be beneficial when reading the analysis. In this section we define the fundamental structures and results from measure theory used in stochastic calculus and the section culminates in the definition of the Itô integral and Itô processes. Proofs have been entirely left out for brevity. The progression followed below is a simplification of that in [Kopp, 2011] and I have used similar notation. The author also consulted [Doob, 1953] and [Bharucha-Reid, 1960] to clarify some concepts. An extremely readable introduction to the preliminary (abstract) measure theory is [Tao, 2011].

In all cases below, Ω is an abstract space of ω points.

Definition A.1 (Field and σ-Field)**.** A class $\mathcal{F}$ of ω sets is called a **field** if it has the following properties:

1. $\Omega \in \mathcal{F}$,

2. if $\Lambda \in \mathcal{F}$, then $\Lambda^c \in \mathcal{F}$,

3. if $n \in \mathbb{N}$ and if $\Lambda_1, \Lambda_2, \ldots, \Lambda_n \in \mathcal{F}$, then

$$\bigcup_1^n \Lambda_j \in \mathcal{F}, \ \bigcap_1^n \Lambda_j \in \mathcal{F}$$

A field is called a σ-**field** if it has the additional property of closure under infinite unions and intersections:

4. if $\Lambda_1, \Lambda_2, \cdots \in \mathcal{F}$, then

$$\bigcup_1^\infty \Lambda_j \in \mathcal{F}, \ \bigcap_1^\infty \Lambda_j \in \mathcal{F}$$

Theorem A.2 (Generated σ-field)**.** *If $\mathcal{F}_0$ is a class of ω sets, there is a uniquely determined σ-field, $\mathcal{F}$ of ω sets with the following two properties*

1. $\mathcal{F}_0 \in \mathcal{F}$;

2. if $\mathcal{F}_1$ is a σ-field of ω sets and if $\mathcal{F}_0 \subset \mathcal{F}_1$, then $\mathcal{F} \subset \mathcal{F}_1$.

We will denote this unique σ-field as $\sigma(\mathcal{F}_0)$ - the σ-field generated by $\mathcal{F}_0$.

In the following we shall discuss the concept of ω functions. Functions defined on various sets of ω points allow us to define sets of ω points as constraints on these functions. Such functions can be real or complex valued.

Definition A.3 (Measurable Space and Measure)**.** The triplet $(\Omega, \mathcal{F}, \mu)$ is called a *measure space* if F is σ-field of subsets of Ω, and if the function $\mu : \mathcal{F} \to [0, \infty]$ has the properties

1. $\mu(\emptyset) = 0$ and

2. for any disjoint sequence (A_n) in $\mathcal{F}$,

$$\mu\left(\bigcup_{n=1}^\infty A_n\right) = \sum_{n=1}^\infty \mu(A_n)$$

.

μ is called a *measure* on the *measurable space* $(\Omega, \mathcal{F})$.

Many measurable spaces allow for more than one type of measure to be defined on them. Hence they can be used to form many different measure spaces.

Definition A.4 (Measurability)**.** A function $f : (\Omega, \mathcal{F}) \to (\Omega', \mathcal{F}')$ is called *measurable* with respect to $\mathcal{F}$ if $f^{-1}(E') \in \mathcal{F}$ for all $E' \in \mathcal{F}'$.

We now mention a particularly important measurable space. Let

$$\mathcal{B}_0 := \left\{ \bigcup_{i=1}^{n} (a_i, b_i] : a_i, b_i \in [-\infty, \infty],\ a_1 \leq b_1 \leq a_2 \leq \cdots \leq b_n,\ n \geq 1 \right\}.$$

We call $\mathcal{B}_0$ the class of all finite unions of disjoint intervals on the extended reals, denoted $\bar{\mathbb{R}} := \mathbb{R} \cup [-\infty, \infty]$. $\mathcal{B}_0$ is in fact a field on $\mathbb{R}$ and the σ-field generated by $\mathcal{B}_0$, denoted $\mathcal{B} = \sigma(\mathcal{B}_0)$, is called the **Borel field**.

For the case of the measurable spaces $(\Omega, \mathcal{F})$ and $(\bar{\mathbb{R}}, \mathcal{B})$ we have an equivalent definition of measurable. The real-valued function $X : \Omega \to \mathbb{R}$ is measurable with respect to $\mathcal{F}$ if, for every $c \in \mathbb{R}$, the ω-set $\{\omega : X(\omega) < c\}$ is in $\mathcal{F}$. See [Kopp, 2011] for a proof of these statements. We call a measure on measurable space $(\Omega, \mathcal{F})$ *finite* if $\mu(\Omega) < \infty$. We call a measure *σ-finite* if there exists a sequence $(F_n)_n$ in $\mathcal{F}$ such that $\mu(F_n) < \infty$ for all n and $\cup_n^\infty F_n = \Omega$.

I now note a few important characteristics of measurable functions. Linear combinations of functions measurable with respect to $\mathcal{F}$ are measurable with respect to $\mathcal{F}$. If $\{X_n, n \geq 1\}$ is a sequence of ω functions each measurable with respect to $\mathcal{F}$, then the set of points on which $\{X_n, n \geq 1\}$ converges, defined as

$$\{\omega_X\} := \left\{ \omega : \lim_{n \to \infty} X_n(\omega) = X_\omega \in R \right\},$$

is in $\mathcal{F}$. If the sequence $\{X_n, n \geq 1\}$ converges everywhere, then its limit is a function measurable with respect to $\mathcal{F}$. An important type of measure spaces are probability spaces, defined as follows:

Definition A.5 (Probability space)**.** The measure space $(\Omega, \mathcal{F}, P)$ is called a **probability space** if P satisfies

1. $P : \mathcal{F} \to [0, 1]$,
2. $P(\Omega) = 1$ and

3. for any sequence (A_n), $(n \in \mathbb{N})$, in $\mathcal{F}$ such that $n \neq m \Rightarrow A_n \cap A_m = \emptyset$, we have that

$$P(\cup_{n=1}^{\infty} A_n) = \sum_{n=1}^{\infty} P(A_n).$$

Important to stochastic calculus is the uniqueness of measures like the Lebesque measure. To discuss this we need a few more definitions.

Definition A.6 (Outer Measure and μ^*-measurable)**.** The function $\mu^* : 2^{\Omega} \to [0, \infty]$ is called an **outer measure** if it satisfies

1. $\mu(\emptyset) = 0$,
2. for any subsets A, B of Ω such that $A \subset B$, we have that $\mu^*(A) \leq \mu^*(B)$, (Monotonicity)
3. for any sequence of subsets $(A_i)_i$, $\mu^*(\cup_{i=1}^{\infty} A_i) \leq \sum_{i=1}^{\infty} \mu^*(A_i)$. (Countably subadditive)

Let μ^* be an outer measure. The set $A \subset \Omega$ is μ^*-measurable if, for each $E \subset \Omega$,

$$\mu^*(E) = \mu^*(E \cap A) + \mu^*(E \backslash A)$$

Consider the function $m : \mathcal{B}_0 \to [0, \infty)$ defined as $m(\cup_{i=1}^{n}(a_i, b_i]) = \sum_{i=1}^{n}(b_i - a_i)$. m is a measure on $\mathcal{B}_0$. Unfortunately, m is not countably additive on $\mathcal{B}$, and hence not a measure on the Borel set, $\mathcal{B}$. We can, though, consider the related outer measure instead, namely

$$m*(E) := inf\left\{\sum_{i=1}^{n}(b_i - a_i) : E \subset \cup_{i=1}^{\infty}(a_i, b_i]\right\}.$$

A key result is the implementation of Carathéodory's Extension Theorem:

Theorem A.7 (Carathéodory extension)**.** *Let $\mathcal{F}_0$ be a field of subsets of the set Ω and let $\mu : \mathcal{F}_0 \to [0, \infty]$ be a measure. Define μ^* as*

$$\mu^*(E) = inf\left\{\sum_{i=1}^{n} \mu(A_i) : A_i \in \mathcal{F}_0, E \subset \cup_{i=1}^{\infty} A_i\right\},$$

for $E \subset \Omega$. Then μ^* and μ agree on $\mathcal{F}_0$, every set in $\mathcal{F}_0$ is μ^*-measurable and, if μ is countably additive on $\mathcal{F}_0$, then μ^* is the unique extension of μ to a measure on the σ-field $\mathcal{F} = \sigma(\mathcal{F}_0)$.

I refer you to [Kopp, 2011] for a brief outline of a proof for this theorem. The key point, though, is that this tells us that the m^* defined earlier is the *unique* extension of m on $\mathcal{B}$. Now let $\mathcal{N}$

be the collection of all $m*$-null sets: $\mathcal{N} := \{N : m*(N) = 0\}$. We then define $\mathcal{L} := \mathcal{B} \cup \mathcal{N}$. $\mathcal{L}$ is called the collection of Lebesque measurable sets. From here on we will write m for m^* which we have defined as Lebesque measure: $m : \mathbb{L} \to [0, \infty]$.

Consider a probability space $(\Omega, \mathcal{F}, P)$. Let $X : (\Omega, \mathcal{F}, P) \to (\mathbb{R}, \mathcal{B})$ be a function measurable with respect to $\mathcal{F}$. Such real-valued functions from a probability space to $(\mathbb{R}, \mathcal{B})$ are called *random variables*. A sequence of random variables, indexed by α, is called a *stochastic process* and is written $((X_\alpha)_{\alpha \in \Lambda})$. It is called *discrete* if the set of indices, Λ, is countable or *continuous* if Λ is uncountable (usually $[0, \infty)$ to represent time).

We then have that the pre-images $X^{-1}(E) \in \mathcal{F}$ for all $E \in \mathcal{B}$ are well defined and we can define the function $P_X : \mathcal{B} \to [0, 1]$ as $P_X(E) = P(X^{-1}(E))$. This new function is, in fact, a probability measure on the measurable space $(\mathbb{R}, \mathcal{B})$. We can make use of our earlier remark that measurable functions with range-space $(\mathbb{R}, \mathcal{B})$ are equally well defined by their values on the set of all intervals of the form $(-\infty, x]$. We use this to define the *distribution function* of a probability as $F_{P_X}(x) := P_X((-\infty, x])$. We call this function the *law* of the random variable X, usually written $F_X(x) = P_X((-\infty, x])$. An equivalent way of describing random variables is by their *characteristic functions*. Every distribution function has a unique characteristic function defined as

$$\phi_X(\lambda) = \mathbb{E}\left[\exp(i\lambda X)\right].$$

If the distribution function is differentiable, it's derivative is called the *probability density function*. In these cases, the characteristic function is in effect the Fourier transform of the density function. Working with characteristic functions is useful because, in several contexts, it allows an easy way to calculate certain quantities, such as moments of the random variable[1].

Another useful concept is that of a σ-field generated by a random variable. We write $\sigma(X) := \{X^{-1}(B) : B \in \mathcal{B}\}$. This can be extended to The σ-field generated by a process, defined as the minimal σ-field which contains all the σ-fields generated by the X_αs.

Product measures are the extension of measures to spaces which are the Cartesian product of two (or more) spaces. Let $(\Omega_1, \mathcal{F}_1)$ and $(\Omega_2, \mathcal{F}_2)$ be two measurable spaces. The *product* $\sigma - field$ $\mathcal{F} = \mathcal{F}_1 \times \mathcal{F}_2$ on the Cartesian product $\Omega = \Omega_1 \times \Omega_2$ is defined as $\mathcal{F} := \sigma(\mathcal{R})$, where $\mathcal{R} = \{F_1 \times F_2 : F_1 \in \mathcal{F}_1,\ F_2 \in \mathcal{F}_2\}$. Another way to think of this is in terms of projection maps. If $\rho_i : \Omega \to \Omega_i$ $(i = 1, 2)$ is a projection map such that $\rho_i(\omega_1, \omega_2) = \omega_i$, we can equivalently define $\mathcal{F}$

[1] Note, the characteristic function is *not* the same thing as the moment generating function! The former always exists whereas the latter may not. A discussion of this is unnecessary for our scope.

as the smallest σ-field over which ρ_1 and ρ_2 are both measurable. Many of our earlier mentioned results and definitions extend naturally to the product measures so their reproduction will be omitted for brevity. We now return to our conventional definition of Ω.

We can now begin to construct integrals over arbitrary spaces with respect to some σ-finite measure μ. First, we define indicator functions and simple functions.

Definition A.8 (Indicator Function)**.** Let $(\Omega, \mathcal{F}, \mu)$ be a fixed σ-finite measurable space. For $A \in \mathcal{F}$, we define the **indicator function** $\mathbf{1}_A : \Omega \to \{0, 1\}$ as

$$\mathbf{1}_A(x) := \begin{cases} 1 \quad if & x \in A, \\ 0 \quad if & x \notin A. \end{cases}$$

Definition A.9 (Simple Function)**.** Let $(\Omega, \mathcal{F})$ be a measurable space. We call the function $\phi : \Omega \to \mathbb{R}$ a **simple function** if it has a finite range: i.e. it takes on only a finite number of values in $\mathbb{R}$. Suppose these n distinct values are $\{a_1, a_2, \ldots, a_n\}$, then we can partition Ω into a finite number of disjoint sets, labelled A_i, in $\mathcal{F}$, defined by $A_i = \phi^{-1}(\{a_i\}) = \{\omega : \phi(\omega) = a_i\}$, for $i = 1, \ldots, n$. Moreover, we can represent $\phi(\omega) = \sum_{i=1}^{n} a_i \mathbf{1}_{A_i}(\omega)$.

Note that the set of all simple functions (for a given measurable space) forms a vector space, denoted $\mathcal{S}(\mathcal{F})$. It is intuitively quite obvious that we can approximate (to arbitrary precision) any measurable function with a series of simple functions. To be particular, consider the following proposition:

Proposition A.10. *Let $(\Omega, \mathcal{F})$ be a measurable space and let $f : \Omega \to [0, \infty)$ be measurable with respect to $\mathcal{F}$. Define the sequences of sets $A_k = f^{-1}([\frac{k-1}{2^n}, \frac{k}{2^n}))$ and $B_k = f^{-1}((k, \infty))$. Then the sequence of simple functions (s_n) for*

$$s_n = \sum_{k=1}^{n2^n} \frac{k-1}{2^n} \mathbf{1}_{A_k} + n\mathbf{1}_{B_n}$$

converges pointwise to f.

We can now begin to define integrals of **positive** measurable functions with respect to some measure.

Definition A.11 (μ-integral)**.** Let $(\Omega, \mathcal{F}, \mu)$ be a fixed σ-finite measure space. For any $A \in \mathcal{F}$ define the μ-integral of its indicator, $\mathbf{1}_A$ as

$$\int_\Omega \mathbf{1}_A(\omega)\mu(d\omega) = \int_\Omega \mathbf{1}_A d\mu := \mu(A).$$

Note the notation of the integral. The integral is over the space Ω and the indicator function is a function of elements of this space. The value of the integral, though, depends principally on the measure, μ, and hence the second, conventional notation. By linearity, we can extend this definition as follows: let $\phi = \sum_{i=1}^n a_i \mathbf{1}_{A_i}$, where $a_i > 0$ and $(A_i)_{i \leq n} \in \mathcal{F}$ are pairwise disjoint. Then we have that

$$\int_\Omega \phi(\omega)\mu(d\omega) = \sum_{i=1}^n a_i \mu(A_i).$$

For the integral of a positive real function with respect to the Lebesque measure m, this becomes more evident: we write $\int_{-\infty}^{\infty} f(x)m(dx)$. For example $\int_{-\infty}^{\infty} \mathbf{1}_{\mathbb{Q}} m(dx) = 1m(\mathbb{Q}) + 0m(\mathbb{R}/\mathbb{Q}) = 0$. Note that we can restrict our integral to an arbitrary subset $E \in \mathcal{F}$ by simply writing $\int_E f d\mu = \int_\Omega (f \cdot \mathbf{1}_E) d\mu$. We want to extend the definition of μ-integrals from the the space of simple functions (measurable on $\mathcal{F}$) to the space of all functions which are $\mathcal{F}$-measurable. We use our earlier statement that all measurable functions can be written as the limit of a sequence of simple functions. So, if we write

$$Y(f) = \left\{ \int_\Omega \phi d\mu : \phi \in \mathcal{S}(\mathcal{F}) : 0 \leq \phi \leq f \right\},$$

we can then define

$$\int_\Omega f d\mu := \sup(Y).$$

The Monotone Convergence Theorem equips us with the stability of these integrals for pointwise convergent sequences of functions. We state it as follows:

Theorem A.12 (Monotone Convergence)**.** *Let $(f_n)_{n \geq 1}$ be a sequence of positive measurable functions which converges pointwise to f on $E \in \mathcal{F}$. Then*

$$\int_E f_n d\mu = \int_E f d\mu \text{ as } n \to \infty.$$

We emphasise the restriction to positive measurable functions because we must avoid integrals which evaluate to $\infty - \infty$. So we restrict ourselves to the space $\mathcal{L}^1(\Omega, \mathcal{F}, \mu) := \{f : \int_\Omega |f| d\mu <$

$\infty\}$. We call $f \in \mathcal{L}^1$ **μ-integrable**. Note this is a slightly stronger requirement than measurability. A function may be measurable but not integrable with respect to μ.

A.1 Stochastic Integrals

The earlier construction of integration of measurable functions with respect to a measure will now help us construct a similar concept for the integration with respect to (continuous) stochastic processes. In defining μ-integrability, we required the notion of point-wise convergence, both of simple functions and then sequences of positive-measurable functions. A similar construction must now occur, where we consider sequences of sub-σ-fields. A sub-σ-field is a σ-field contained by the σ-field generated by the whole possible state space, Ω. A natural and useful example is taken for stochastic processes. Suppose we have the stochastic process $(X_\alpha)_{\alpha\in\mathbb{N}}$. The σ-field generated by the sub-process $(X_\alpha)_{\alpha\leq 3}$ is a sub-σ-field of the σ-field generated by the whole process. This leads naturally to the definition of *filtrations*. First, though, we must define the concept of conditional expectation. We assume the reader is comfortable with the expectation of a random variable: for probability space $(\Omega, \mathcal{F}, P)$, the expectation value of $X : \Omega \to \mathbb{R}$ is denoted $\mathbb{E}[X] := \int_\Omega X dP$.

To define conditional expectation, we need to account for the fact that different random variables in $\mathcal{L}^1$ could be indistinguishable almost surely in P. To avoid this, we work in the quotient space attained by identifying random variables into equivalence classes when they agree almost surely on P. This gives us Banach space structure. Let us fix a probability space $(\Omega, \mathcal{F}, P)$. In a natural re-use of the notation used earlier[2], we let $\mathcal{L}^p = \{X : \Omega \to \mathbb{R} : \mathbb{E}[|X|^p] < \infty\}$, for $p \geq 1$. For a given value of p, $||\cdot||_p : X \to (\mathbb{E}[|X|^p])^{1/p}$ defines a norm so we can define equivalence classes as $X \sim Y$ if and only if $X = Y$ almost surely in P, or (equivalently) $||X - Y||_p = 0$. By identifying random variables which are in the same equivalence class we form the quotient space, denoted $L^p(\Omega)$, or L^p. This is a Banach space, which is important for the following definition in which $p = 1$.

Definition A.13 (Conditional Expectation)**.** If $X \in L^1(\Omega, \mathcal{F}, P)$ and $\mathcal{G}$ is a sub-σ-field of $\mathcal{F}$, then the **conditional expectation** of X given $\mathcal{G}$ is the G-measurable random variable $\mathbb{E}[X|\mathcal{G}]$, such that $\int_G \mathbb{E}[X|\mathcal{G}]dP = \int_\mathcal{G} X dP$ for all $G \in \mathcal{G}$.

Definition A.14 (Filtrations and Martingales)**.**

[2]Recall we used $\mathcal{L}^1$ to denote the space of μ-integrable functions. Here we are specifying that μ must be a probability measure and we are considering the more general case of the p-norm.

- Let $\mathbb{F} = (\mathcal{F}_i)_{i\geq 0}$ be an **increasing** sequence of sub-σ-fields. We call $\mathbb{F}$ a **filtration**. The sequence of random variables $(X_\alpha)_{\alpha\geq 0}$ is **adapted** to $\mathbb{F}$ if, for each n, X_n is $\mathcal{F}_n$ measurable. $(\Omega, \mathcal{F}, \mathbb{F}, P)$ is called a *filtered space*.

- The adapted sequence $(X_n, \mathcal{F}_n)$ is called a $(\mathbb{F}, P)$**-martingale** if each X_n is integrable and

$$\mathbb{E}[X_n|\mathcal{F}_{n-1}] = X_{n-1} \text{ almost surely in } P \text{ for each } n \geq 1.$$

We now bring several of these concepts together. A naturally common stochastic process of interest is the continuous process $X = (X_t)_{t\in\mathbb{T}}$, where $X_t : \Omega \to \mathbb{R}$ and $[0, \infty) =: \mathbb{T}$ represents time. Similarly, we can see this as a random variable on a product space $X : \mathcal{T} \times \Omega \to \mathbb{R}$. This map is measurable if $X^{-}1(B) \in \sigma(\mathcal{B}_\mathbb{T} \times \mathcal{F})$ for every Borel set B. $\mathcal{B}_\mathbb{T}$ denotes $\mathcal{B} \cap \mathbb{T}$. We will also be working in the normed space L^2 for the following reasons. As will be evident later, we are often interested in how well two random variable "agree". Suppose we want to characterise how "close" two random variables (X and Y)are on some sub-σ-field. Calculating $||X - Y||_2^2 = \mathbb{E}\left[|X - Y|^2\right] = \mathbb{E}[X^2 - 2XY - Y^2]$ amounts to calculating variances of X and Y and Hölder's inequality (see [Kopp, 2011, p. 50]) tells us that $\mathbb{E}[XY] \leq ||X||_2||Y||_2$, where equality holds if X and Y are independent. Minimisation in the L^2-norm is what statisticians called the "least-squares" fit and is optimal for processes with non-zero finite variances.

We now define a very important example of such a process.

Definition A.15 (Wiener Process)**.** Let $(\Omega, \mathcal{F}, P)$ be a probability space. The stochastic process $B : \mathbb{T} \times \Omega \to \mathbb{R}$ is called a **Wiener process** if:

1. $B(0, \omega) = 0$ almost surely in P,
2. for $0 \leq s < t < \infty$, the random variable $\Delta B := B(t, \omega) - B(s, \omega)$ is normally distributed, with mean 0 and variance $(t - s)$,
3. for $m \in \mathbb{N}$ and the disjoint intervals $0 \leq t_1 < t_2 < \ldots < t_m$, the increments $\Delta B_i = B(t_{i+1}, \omega) - B(t_i, \omega)$ are independent,
4. the paths $t \to B(t, \omega)$ are continuous almost everywhere in P.

The term Brownian Motion is often used for the Wiener process. Here we make a slight distinction. It is of little use considering the process B itself. Most often we make use of the convention that $B(0, \omega) = 0$ a consider the random variable $B_t(\omega) := B(t, \omega) - B(0, \omega)$. We will call this

Brownian Motion (BM). B_t is then normally distributed around 0 with variance t. The Wiener process/Brownian motion is a fundamental and thoroughly studied construction. A discussion of all its known properties would be a chapter on its own. We mention it here because it is used in constructing the canonical stochastic integral, the Itô integral. To do so though, it is useful to note some properties of BM. The characteristic function of BM can be calculated as follows

$$\begin{aligned}\phi_{B_t}(\lambda) =&\mathbb{E}[\exp(i\lambda B_t)] = \int_{-\infty}^{\infty} \exp(i\lambda x)\exp(-\frac{x^2}{2t})dx \\ =&\exp(-\frac{t}{2}\lambda^2).\end{aligned} \tag{A.1}$$

This is useful, as we can calculate higher-order moments of BM using the relation $i^n\mathbb{E}[X^n] = \frac{d^n}{d\lambda^n}\phi_X(\lambda)|_{\lambda=0}$. In particular, we note that

$$\mathbb{E}[B_t^4] = \frac{d^4}{d\lambda^4}\exp(-\frac{t}{2}\lambda^2)|_{\lambda=0} = 3t^2.$$

Similarly to how we built integrals with respect to measures in terms of simple functions, we use the notion of a *simple* $\mathbb{F}$*-adapted process* to "build" integrals. We define these as follows:

Definition A.16. Let h be an $\mathcal{F}$-adapted process on $[0,T]\times\Omega$. We say that h is **simple** if, for some partition $\{0 = t_0 < t_1 < t_2 < \ldots < t_n = T\}$ and for the $\mathcal{F}_{t_i}$-measurable random variables $(h_i)_{i<n}$, we have that h_t satisfies

$$h_t(\omega) = \sum_{i=0}^{n-1} h_i(\omega)\cdot \mathbf{1}_{(t_i,t_{i+1}]}(t) \text{ for } 0\le t\le T,\ \omega\in\Omega.$$

Here, $\mathbf{1}_{(t_i,t_{i+1}]}(t)$ is a step function, evaluating to 1 only on the interval $(t_i, t_{i+1}]$. For now, we will restrict ourselves to the class of finite **square** integrable (simple) processes. We will denote this vector space of simple processes in $\mathcal{L}^2$ as

$$\mathcal{H}^2_{[0,T]} := \{h : h \text{ is simple and } h_i \in L^2(\mathcal{F}_{t_i}) \text{ for all } i \le n.\}$$

We can then define Itô integrals of such processes.

Definition A.17 (Itô Integral of a simple process)**.** Let h be a simple process where $h_i \in L^2(\mathcal{F}_{t_i})$ for all $i \le n$. The Itô integral of h, denoted $\int_0^T h_s dB_s$, is defined as

$$\int_0^T h_s dB_s := \sum_{i=0}^{n-1} h_i\cdot(B_{t_{i+1}} - B_{t_i}).$$

Earlier we extended our definition of the μ-integral from positive simple functions on $\mathcal{F}$ to all measurable functions on $\mathcal{F}$. We would like to extend this definition similarly, to include a more general class of measurable processes. For clarity we define the vector space:

$$\mathcal{M}^2_{[0,T]} := \left\{ f : f \text{ is } \mathbb{F}\text{-adapted}, \mathbb{E}\left[\int_0^T f_t^2 dt\right] < \infty \right\}.$$

Note we maintain the convention of denoting the dependence on the σ-field $\mathbb{T}$ as a subscript. It is important to remember that this too is an argument of f as f acts on a product space. The space $\mathcal{M}^2_{[0,T]}$ is equipped with a natural norm due to the fact that it's elements are L^2-processes. We denote and define this norm as

$$||f||_{\mathcal{M}^2_{[0,T]}} := \sqrt{\mathbb{E}\left[\int_0^T f_t^2 dt\right]},$$

which, of course, applies to $\mathcal{H}^2_{[0,T]}$ as well. We will not explicitly prove it here, but it is perhaps not surprising to know that, for any process in $\mathcal{M}^2_{[0,T]}$, there exists a sequence of simple processes in $\mathcal{H}^2_{[0,T]}$ which converges to f in the $\mathcal{M}^2_{[0,T]}$-norm. This means $\mathcal{M}^2_{[0,T]}$ is the *closure* of $\mathcal{H}^2_{[0,T]}$ in the $\mathcal{M}^2_{[0,T]}$-norm. We keep this in mind and note two important results for Itô integrals of simple processes:

Theorem A.18 (Itô isometry)**.**

1. $\mathbb{E}\left[\int_0^T h_t dB_t\right] = 0,$
2. $\mathbb{E}\left[\left(\int_0^T h_t dB_t\right)^2\right] = \mathbb{E}\left[\int_0^T h_t^2 dt\right]$ *- the Itô isometry.*

The Itô isometry tells us something important. Note that on the left hand side, we have the square of the $||\cdot||_2$-norm of the Itô integral. On the right hand side we have the square of the $||\cdot||_{\mathcal{M}^2_{[0,T]}}$-norm of the simple process in $\mathcal{H}^2_{[0,T]}$. The continuity of this map allows us to define the Itô integral for processes in $\mathcal{M}^2_{[0,T]}$ as the limit of the integral of the sequence of processes in $\mathcal{H}^2_{[0,T]}$ which converge to f in the $\mathcal{M}^2_{[0,T]}$-norm.

Definition A.19 (Itô integral)**.** Let $f \in \mathcal{M}^2_{[0,T]}$, and let $h \in \mathcal{H}^2_{[0,T]}$ satisfy

$$\lim_{n\to\infty} ||h_n - f||_{\mathcal{M}^2_{[0,T]}} = 0,$$

everywhere in $\mathcal{T}$. Then we define

$$\int_0^T f_t dB_t := \lim_{n\to\infty} \int_0^T (h_n)_t dB_t.$$

The above limit is well defined and, what's more, it can be shown that, for each $f \in \mathcal{M}^2_{[0,T]}$ we can construct the appropriate sequence of simple processes using indicator functions.

The Itô isometry is even more useful though. It allows us to extend the results in theorem A.18 to functions in $\mathcal{M}^2_{[0,T]}$:

Theorem A.20. *For $f \in \mathcal{M}^2_{[0,T]}$, we have that:*

$\mathbb{E}\left[\int_0^T f_t dB_t\right] = 0,$

$\mathbb{E}\left[\left(\int_0^T f_t dB_t\right)^2\right] = \mathbb{E}\left[\int_0^T h_t^2 dt\right].$

We use this to make an interesting observation. Brownian Motion (for $t \in [0,T]$) is in $\mathcal{M}^2_{[0,T]}$. So what is $\int_0^t B_s dB_s$? We can now calculate this as follows. We partition $[0,t]$ into $n-1$ intervals where $t_0 = 0$, $t_n = s$. Consider the sequence of simple processes $h_n := \sum_{j=0}^{n-1} B_{t_j}\left(B_{t_{j+1}} - B_{t_j}\right)$.[3] Using the identity $a(b-a) = \frac{1}{2}\left((b^2-a^2) - (b-a)^2\right)$, we write

$$h_n = \frac{1}{2}\sum_{j=0}^{n-1}\left((B^2_{t_{j+1}} - B^2_{t_j}) - (B_{t_{j+1}} - B_{t_j})^2\right).$$

We can take the first term outside of the sum, since $\sum_{i=0}^{n}(a_{i+1} - a_i) = a_{n+1} - a_0$. We also have by convention that $B_0 = 0$, so

$$h_n = \frac{1}{2}\left(B^2_{t_n} - \sum_{j=0}^{n-1}(B_{t_{j+1}} - B_{t_j})^2\right).$$

The term in the summation is the variance of the increment $B_{t_{j+1}} - B_{t_j}$. As stated in the definition of the Wiener process these increments are stationary and independent. Furthermore, the sum of all the variances is simply the variance of the overall process. So we have

$$\sum_{j=0}^{n-1}(B_{t_{j+1}} - B_{t_j})^2 = \sum_{j=0}^{n-1}(t_{j+1} - t_j) = t_n.$$

[3] Note that the values of each t_j are in fact n dependent, since for different partitions the edges of the partitions will differ. This is a subtle detail so the notation has been omitted but the reader should be aware.

In the limit $n \to \infty$, h_n converges to $\frac{1}{2}\left(B_s^2 - s\right)$ in the L^2-norm, so by theorem A.19, we have the result

$$\int_0^T B_s dB_s = \frac{1}{2}(B_T^2 - T),$$

a new stochastic process! This result is the basis of the Itô calculus, a stochastic calculus. The Itô integral does not obey the same "rules" as the Riemann or Lebesque integrals. The reason for this difference lies in the integrator, dB_s which has "non-vanishing quadratic variation". Itô processes are stochastic processes which can be written as the (finite) sum of Lebesque and Itô integrals, i.e of the form

$$X_t = X_0 + \int_0^t K_s ds + \int_0^t H_s dBs.$$

It is from these rules and structures of Itô calculus that we can manipulate the compound Poisson processes and other stochastic processes which appear in the following chapter.

Note that is has become a common convention to write equations like that above in derivative form, namely:

$$\dot{X}_t = K_s t + H_t \frac{dB_s}{ds}|_{s=t}. \tag{A.2}$$

This expression is not necessarily well defined - we do not have that dB_s is differentiable with respect to t. We only know that increments of B are normally distributed around 0. The convention is widespread though now and worth noting.

Appendix B

Markov Processes

In analysing spiking network models, it is extremely useful to have some means of approximating distributions of inter spike intervals. This amounts to solving the "first exit time" problem for a stochastic process. To this end, I present below the derivation outlined in [Tuckwell, 1988]. This analysis draws on that of Goldstein and Mandelbrot (1964).

We begin by considering a simple case of a "birth-and-death" process. Consider the function

$$V(t) := N_E(t) - N_I(t)$$

where $N_E(t)$ and N_I are independent Poisson processes with rates λ_E and λ_I respectively. We could say process $V(t)$ has received $N_E(t)$ "excitatory" and N_I "inhibitory" inputs in time interval $[0, t)$.

Note that in the more thorough notation for stochastic processes used in the previous chapter, V would be written as a continuous sequence of random functions $V_t(\omega)$ or as a random variable on a product space: $V(t, \omega)$. In this chapter, the state-space will be known to be the real line. Since (by definition) we do not know what V_t looks like, we can at most make statements about probabilistic measures of pre-images of V - i.e. the likelihood that V_t is *in* some element of the σ-field of the state space (in this case, the Borel field). For this reason, the dependence on the state space is depressed and we write random variables as maps from the index space $\mathbb{T} = [0, \infty)$ to the real line.

The process V is a Markov process: the probability of the random variable being in state y at time t_2 is completely defined by our knowledge that it is in state x at time $t_1 < t_2$. We

do not need to know what trajectory it took *before* then to get to state x. If such a process is continuous in time and discrete in space it is called a *discontinuous Markov process.* Jumps due to new instances ("arrivals") on either of these processes are of magnitude one. Hence N_E and N_I are "jump" processes, where different jumps are statistically independent and the probability distributions of N_E and N_I are Poisson distributions.

Assuming such a process begins at $V(0) = 0$, we would like to know some distribution of the expected value of $V(t)$ for $t > 0$. Consider what would happen in time interval $(t, t + \Delta t]$: the probability that $N_E(t)$ increases is $\lambda_E \Delta t$ and similarly for N_I. The various times at which $V(t)$ changes is thus a Poisson process with mean rate $\lambda = \lambda_E + \lambda_I$. We seek

$$p_m(t) = Pr\{V(t) = m | V(0) = 0\},$$

where $m \in \mathbb{Z}$. This is the conditional probability that $V(t) = m$ given that $V(0) = 0$, known as the *transition probability.* Our derivation thus far considers all trajectories via which $V(t)$ may attain m. In particular, it may have taken $n \geq m$ steps to get there. Furthermore, suppose n_E of these jumps were excitatory (+1) and n_I inhibitory (-1). With this in mind, we can write that, after n jumps,

$$Pr(V = m | V(0) = 0) = \binom{n}{\frac{n+m}{2}} p^{(m+n)/2} q^{(n-m)/2},$$

where $p = \frac{\lambda_E}{\lambda}$, $q = \frac{\lambda_I}{\lambda}$ and $n = n_E + n_I$, $m = n_E - n_I$.

By the law of total probability, we can multiply this by the probability of n jumps occurring in the same time interval, (0,t]: $\frac{e^{-\lambda t}(\lambda t)^n}{n!}$. Using $n = m + 2n_I$, we get

$$p_m(t) = e^{-\lambda t} \sum_{n_I=0}^{\infty} \frac{(\lambda t)^{m+2n_I}}{(m + 2n_I)!} \binom{m + 2n_I}{m + n_I} p^{m+n_I} q^{n_I} \tag{B.1}$$

We we express this more succinctly using the modified Bessel function, defined as

$$I_z(x) := \sum_{k=0}^{\infty} \frac{1}{k! \Gamma(k + z + 1)} \left(\frac{x}{2}\right)^{2k+z},$$

where $\Gamma(k) = (k - 1)!$ is the Gamma function. We obtain

$$p_m(t) = \left(\frac{\lambda_E}{\lambda_I}\right)^{m/2} e^{-\lambda t} I_m(2t\sqrt{\lambda_E \lambda_I}). \tag{B.2}$$

B.1 Thresholds

Consider a trajectory of the process V which we know began at $V(0) = 0$ and ends at $V(t) = m > \theta$. We know that V must have crossed $\theta > 0$ at some point and, in particular, done so for the first time at some $t' < t$. We define the **distribution of first-passage times**:

$$f_\theta(t) := Pr\{V(t) = \theta | V(0) = 0 \ \& \ V(t') < \theta \ \forall \ t' < t\}.$$

Note that this Markov processes is *temporally homogeneous*: i.e it only depends on *differences* in time, not absolute time. We can then integrate over all such possible paths[1] (i.e. crossing θ at all possible t's) and write

$$p_m(t) = \int_0^t f_\theta(t') p_{m-\theta}(t - t') dt' \tag{B.3}$$

In solving for $f_\theta(t)$, we denote the Laplace transform of a function $g(t)$ as $\mathcal{L}(g(t))(s) = g_L(s)$. Under the transform, equation (B.3) can be rearranged into

$$f_{\theta,L}(s) = \frac{p_{m,L}(s)}{p_{m-\theta,L}(s)}.$$

Implementing our earlier expression for $p_m(t)$ (equation (B.1)) and the known Laplace transform:

$$\mathcal{L}(e^{-\lambda t}(\lambda t)^k = \lambda^k (s + \lambda)^{-(k+1)} k!,$$

we obtain

$$f_{\theta,L}(s) = \frac{\lambda^\theta p^\theta}{(s+\lambda)^\theta} \frac{\sum_{n_I=0}^{\infty} \left(\frac{\lambda pq}{(s+\lambda)^2}\right)^{n_I} \binom{m+2n_I}{m+n_I}}{\sum_{n_I=0}^{\infty} \left(\frac{\lambda pq}{(s+\lambda)^2}\right)^{n_I} \binom{m-\theta+2n_I}{m-\theta+n_I}},$$

the inverse Laplace transform of which is

$$f_\theta(t) = \theta \left(\frac{\lambda_E}{\lambda_I}\right)^{\theta/2} \frac{e^{-(\lambda_E+\lambda_I)t}}{t} I_\theta(2t\sqrt{\lambda_E \lambda_I}), \quad t > 0, \tag{B.4}$$

where I_θ is again the modified the Bessel function.

This construction shows that when we consider a simplistic model neuron with no internal dynamics, only a threshold and Poissonian inputs, it is possible to derive a closed expression for the distribution of firing times. We now look at an extension to these "random walk" processes

[1] The Chapman-Kolmogorov identity

in which the random variable representing membrane potential is also effected by self-dependant dynamics.

B.2 Diffusion and Jump-Diffusion Processes

The discrete nature of the above model is obviously quite insufficient in representing the membrane potential of even a simple integrate and fire neuron. To this end we look to the work of Stein (1965) who studied models of diffusive Markov processes. Let $X(t)$ be a random variable of a Markov process, parameterised by continuous time. Suppose at time s, $X(s)$ has the value x. The Markov process random variable, $X(t)$, is fully characterised by the *transition probability distribution function*

$$P(y,t|x,s) = Pr\{X(t) \leq y|X(s) = x\}$$

Because these processes are continuous in t, we can also characterise them through the *infinitesimal generator* ($\mathcal{A}$), which describes transitions of the process over infinitesimal time intervals. For a function f of X which is also continuous with compact support, we define

$$(\mathcal{A}f)(x,t) := \lim_{\Delta t \to 0^+} \frac{\mathrm{E}[f(X(t+\Delta t) - f(X(t))|X(t) = x]}{\Delta t}$$

If the diffusion process concerned is temporally homogeneous, we can simply write $(\mathcal{A}f)(x) = (\mathcal{A}f)(x,t)$, since the infinitesimal transition probability only depends on the *current* position and such transitional probabilities do not change in time.

Diffusion processes are continuous time Markov processes with *continuous state paths*. Their infinitesimal generators can thus be written using their infinitesimal mean ($\alpha(x)$) and variance ($\beta^2(x)$):

$$(\mathcal{A}f)(x) = \alpha(x)\frac{df}{dx} + \frac{\beta^2(x)}{2}\frac{d^2f}{dx^2}, \tag{B.5}$$

where

$$\begin{aligned} \alpha(x) &= \lim_{\Delta t \to 0^+} \frac{\mathrm{E}[X(t+\Delta t) - X(t)|X(t) = x]}{\Delta t} \\ \beta^2(x) &= \lim_{\Delta t \to 0^+} \frac{\mathrm{Var}[X(t+\Delta t) - X(t)|X(t) = x]}{\Delta t} \end{aligned} \tag{B.6}$$

If the variance of the Markov process is bounded over finite intervals in $\mathbb{T}$ then it can then be described by the corresponding stochastic integral or differential equations:

$$X(t) = X_0 + \int_0^t \alpha(X(t'))dt' + \int_0^t \beta(X(t'))dW(t'),$$

where $X(0) = X_0$ is the initial condition, the first integral is a Riemann integral and the second is a *stochastic integral* with respect to the standard Wiener process, W.

Now we can begin to consider jump-diffusion processes ([Tuckwell, 1988, p. 147]). Consider a random Markov process, $X(t)$, that experiences jumps of *various* magnitudes. Suppose all such magnitudes are in the set A. Let $v(t, A)$ be the number of jumps of X up until time t which have magnitudes in A[2]. If the A_i's are disjoint sets (for $i = 1, 2, 3..., n$) then $v(t, A_1), v(t, A_2), ..., v(t, A_n)$ are mutually independent processes. Integrating over all jump amplitudes regains the original process:

$$X(t) = \int_{\mathbb{R}} uv(t, du). \tag{B.7}$$

If this process is in turn the input to a Markov diffusion process, we can write down the following stochastic integral equation for the resultant Markov process:

$$X(t) = X(0) + \int_0^t \alpha(X(t'))dt + \beta(X(t'))dW(t') + \int_0^t \int_{\mathbb{R}} \gamma(X(t'), u)v(dt', du). \tag{B.8}$$

More often though (and somewhat less rigorously) the differential form of this equation is written down:

$$dX = \alpha(X)dt + \beta(X)dW + \int_{\mathbb{R}} \gamma(X, u)v(dt, du). \tag{B.9}$$

$\gamma(X, u)$ is a real-valued measurable function on the compound measure space $(\mathbb{R}, \mathcal{B}) \times (\mathbb{R}, \mathcal{B})$. It is essentially a scaling function, as the effects of jumps may be dependent on the current state. More usefully said, $\gamma(X, u)$ is a "weighting" coefficient which describes the magnitude of the effect of jumps of different sizes given the state of the process at the moment of that jump's arrival.

Now consider the restricted case where for each fixed A, $v(t, A)$ is a temporally homogeneous Poisson process with mean rate $\Pi(A)$ - the rate being A dependant. Π is in fact a *rate measure* on the σ-field of all A's. We then have that $E[v(t, A)] = t\Pi(A)$. The unique *rate density* is

[2]In relation to appendix A, v is a measure on a compound measure space. In particular, it is measure over the σ-field generated by the set of all subsets of jump sizes - all possible As.

defined as $\pi(u)$, where

$$\Pi(du) = \pi(u)du.$$

and the process has a total jump rate of

$$\Lambda = \int_{\mathbb{R}} \pi(u)du.$$

For this scenario, the process, $X(t) = \int_{\mathbb{R}} uv(t, du)$, is called a *compound Poisson process*. In this setting, it can be shown that the infinitesimal generator for the resultant Jump-Diffusion process is

$$(\mathcal{A}f)(x) = \alpha(x)\frac{df}{dx} + \frac{\beta^2(x)}{2}\frac{d^2f}{dx^2} + \int_{\mathbb{R}} f(x + \gamma(x, u))\Pi(du) - \Lambda f \tag{B.10}$$

As a simple example, we take a Brownian motion with drift as our drift-diffusion process (i.e. constant α and β) with a random walk like that mentioned earlier as our jump process. The jumps have magnitudes 1 and -1 at rates λ_+ and λ_- respectively. This has can be written in the stochastic integral form as

$$X(t) = X(0) + \alpha t + \beta W(t) + N_+(t) - N_-(t),$$

where $N_+(t)$ and $N_-(t)$ are the values of the Poisson processes at time t. We want to know what the infinitesimal generator of such a process is, so we note that

$$\pi(u) = \lambda_+\delta(u - 1) + \lambda_-\delta(u + 1) \tag{B.11}$$

$$\Rightarrow \Lambda = \int_{\mathbb{R}} \pi(u)du = \lambda_+ + \lambda_-. \tag{B.12}$$

γ is simple: independent of X, as the size of jumps is independent of the state of the process and taking magnitude of the jumps themselves. Hence $\gamma(X, u) = u$. The associated infinitesimal generator is then

$$(\mathcal{A}f)(x) = \alpha\frac{df}{dx} + \frac{\beta^2}{2}\frac{d^2f}{dx^2} + (\lambda_+ f(x + 1) + \lambda_- f(x - 1)) - (\lambda_+ + \lambda_-)f(x). \tag{B.13}$$

B.3 First exit times

Consider such a compound Poisson process on the real line with initial condition $X(0) = x \in [a, b]$. The random variable

$$T_{ab}(x) := \inf\{t | X(t) \notin (a, b),\ X(0) = x\}$$

will have some distribution function, say

$$F_{ab}(x, t) := Pr\{T_{ab}(x) \leq t\}.$$

Taking the derivative of this distribution function with respect to time, we can define a probability density function of the first exit time from (a, b):

$$\int_{-\infty}^{t} f_{ab}(x, t')dt' := F_{ab}(x, t),$$

$$f_{ab}(x, t) = \frac{\partial F_{ab}}{\partial t}(x, t).$$

[Tuckwell, 1976] showed that, for a diffusion process, this density function obeys

$$\frac{\partial f_{ab}}{\partial t}(x, t) = (\mathcal{A} f_{ab})(x, t),\ \text{for } x \in (a, b),\ t > 0,$$

with boundary conditions

$$f_{ab}(x, 0) = 0, \quad x \in (a, b)$$

$$f_{ab}(x, t) = \delta(t), \quad x \notin (a, b).$$

The n^{th} moment of the first exit times (about the origin) is defined as

$$\mu_{n,ab}(x) = \int_0^\infty t^n f_{ab}(x, t)dt, \quad \text{for } n \in \mathbb{Z}^+.$$

and, as shown in [Darling and Siegert, 1953] and [Tuckwell, 1976], higher-order moments obey the recurrence relation

$$(\mathcal{A}\mu_{n,ab})(x) = -n\mu_{n-1,ab}(x). \tag{B.14}$$

For the particular case of first exit times from the interval $(-\infty, b)$ we consider the limit $a \to -\infty$.

B.4 Stein's Model

[Stein, 1965, Stein, 1967] considered the random variable of a single neuron's membrane potential, $X(t)$, for $t \geq 0$. For subthreshold dynamics ($X < \theta$), the variable would change by jumps due to inputs of, potentially, various magnitudes, such as in equation (B.7). At the same time, the membrane potential will always tend to decay back to its resting value. Hence this variable obeys the stochastic differential equation

$$dX = -X dt + \int_{\mathbb{R}} uv(dt, du), \text{ for } t > 0, \ X < \theta.$$

He then considered the scenario where the neuron receives input form only two sources, one causing positive jumps in X of size a_E and one causing negative jumps in X of size a_I. We could express this via the rate density function: equation (B.11). By equation (B.10), we can now calculate the infinitesimal generator of this process, namely

$$(\mathcal{A}f)(x) = -x\frac{df}{dx} + \lambda_E f(x + a_E) + \lambda_I f(x - a_I) - (\lambda_E + \lambda_I) f(x). \tag{B.15}$$

From the recursion relation between moments of the first-exit times of Markov processes, equation (B.14), we have the following relationship between moments of the first-exit times of this process

$$-n\mu_{n-1,ab} = -x\frac{d\mu_{n,ab}}{dx} + \lambda_E \mu_{n,ab}(x + a_E) + \lambda_I \mu_{n,ab}(x - a_I) - (\lambda_E + \lambda_I)\mu_{n,ab}(x). \tag{B.16}$$

This system can be solved for a few specific cases (e.g. $\lambda_I = 0$, see [Tuckwell, 1988]). In the case of the I-&-F neuron, we would need to consider solutions with boundary conditions at $a \to -\infty$. This was the case for equation (2.16).

Appendix C

The Diffusive Limit

The diffusive limit in the context of a network of I-&-F neurons refers to two reasonable approximations in the limit of large number of inputs of small amplitude. The first is the **central limit theorem:** that a random variable consisting of sampling a large number of independent (Poisson or other) random processes will tend to follow a Gaussian distribution. The second is that a random walk (or stochastic process) consisting of an extremely large number of extremely small discrete steps is an essentially continuous process. Informally speaking, diffusion processes (or rather, Itō diffusion processes) are stochastic processes where the (random) state variable is a continuous function of the time parameter.

C.1 Diffusive limit of a spiking network

Consider the case of a neuron receiving randomly distributed, discrete spikes on dendritic inputs. Arrival of each spike causes a pulse of input current at the soma of finite size. Once such an input current arrives, the total current decays back to zero at a characteristic rate, τ'. The total input current to such a neuron (at the soma) would thus be the stochastic process described by

$$\tau' \frac{dI}{dt} = -I(t) + \Delta I \sum_{j=1}^{N} J'_j \delta(t - t_j^k - d_j), \tag{C.1}$$

where t_j^k is the k^{th} spike time of the j^{th} afferent neuron and d_j is the "transmission delay" on the axon and dendrites. J'_j is a dimensionless magnitude of input from afferent neuron j and

would depend on strength of the synapse and proximity to the soma. ΔI is a constant scaling parameter.

We can rewrite this in approximate difference form

$$I(t+\Delta t) - I(t) \approx -\Delta t \frac{I(t)}{\tau'} + \Delta t \frac{\Delta I}{\tau'} \sum_j J'_j \Delta N_j(\Delta t), \tag{C.2}$$

where Δt is a small enough interval of time such that $I(t+\Delta t) - I(t)$ can be expected to be very small. $\Delta N_j(\Delta t)$ is the number of inputs arriving on connection j in the interval Δt. This is obviously a strongly fluctuating quantity, but in the case that the afferent sources are Poisson processes of fixed rate, we can write

$$E[\Delta N_j(\Delta t))] = \nu_j \Delta t,$$

where E denotes the expected value and ν_j is the rate of j^{th} afferent Poisson process.

Averaging equation (C.2) over a small time interval δt for $\delta t < \Delta t$, to smooth out fluctuations, we then divide by Δt:

$$\frac{\bar{I}(t+\Delta t) - \bar{I}(t)}{\Delta t} = -\frac{\bar{I}(t)}{\tau'} + \Delta t \frac{\Delta I}{\tau'} \sum_j^N J'_j \nu_j(t),$$

which, if $\Delta t << \tau'$, we can approximate as

$$\tau' \frac{d\bar{I}}{dt}(t) = -\bar{I}(t) + \Delta t \Delta I \sum_j^N J'_j \nu_j(t). \tag{C.3}$$

The argument above depends critically on the separation of time scales. For arguments as to its validity for a model of cortical conditions, see Frolov [Frolov and Medvedev, 1986] and Amit and Tsodyks [Amit and Tsodyks, 1991]. In the main text, the over bar notation to indicate the infinitesimal averaging of I is dropped. In moving to the Brunel model and hence equation (1.4), we again restrict ourselves to the case that $\tau' << \tau$, so that, for the purposes of timescales in equation (1.3), equation (C.3) can be written

$$\bar{I}(t) = \Delta t \Delta I \sum_j^N J'_j \nu_j(t). \tag{C.4}$$

Equation (1.4) is just such a case, with scaling parameter $J_j := R\Delta I J'_j$ and $\Delta t \to \tau$. The input to each neuron can thus be written as a sum of scaled Poisson processes with rates ν_j.

C.2 Gaussian approximation to sum of Poisson processes

Consider N independent Poisson processes with rates (and hence variances) λ_i. If we consider $\mathrm{E}[n(\tau)]$, the expected number of total instances on all these processes in time interval $(t, t+\tau]$, we have $\mathrm{E}[n(\tau)]=(\sum_{i=1}^{N}\lambda_i)\tau$. Similarly, the variance in the resultant compound Poisson process is $\mathrm{Var}[n(\tau)]=(\sum_{i=1}^{N}\lambda_i)\tau$. Let $\sum_{i=1}^{N}\lambda_i =: \lambda$. We can now consider the case when, although each process has a fairly low rate ($\lambda_i < 10$ Hz), there are very many processes ($N \to \infty$) and so λ is large. Let $x := \lambda(1+\delta)$ where $|\delta| << 1$. The probability of x occurrences in a unit time is then

$$P(\lambda(1+\delta)) = \frac{\lambda^{\lambda(1+\delta)}e^{-\lambda}}{\sqrt{2\pi}e^{-\lambda(1+\delta)}[\lambda(1+\delta)]^{\lambda(1+\delta)+\frac{1}{2}}}$$

$$= \frac{e^{\lambda\delta}(1+\delta)^{-\lambda(1+\delta)-\frac{1}{2}}}{\sqrt{2\pi\lambda}}.$$

Note that $\ln[(1+\delta)^{\lambda(1+\delta)+\frac{1}{2}}] = (\lambda(1+\delta)+\frac{1}{2})\ln[1+\delta]$ and $\ln[1+\delta] \approx \delta - \delta^2/2 + \mathbf{O}(\delta^3)$. Hence

$$P(\lambda(1+\delta)) \approx \frac{e^{-\lambda\delta^2/2}}{\sqrt{2\pi\lambda}},$$

and substituting back for $\delta = (x-\lambda)/\lambda$,

$$P(x) \approx \frac{e^{-(x-\lambda)^2/(2\lambda)}}{\sqrt{2\pi\lambda}},$$

so, x is normally distributed with mean λ and variance λ. Note that, by it's above definition, x is a fluctuation from the mean, λ. Hence it is these fluctuations which are normally distributed and we can describe an input consisting of these N independent processes as $\lambda(t) + \sqrt{\lambda(t)}\eta(t)$, where $\eta(t)$ is a normally distributed white noise process with zero mean and unit variance. Note that if the jumps or impulses on process i are scaled by magnitude a_i, we would have $\mathrm{E}[n(\tau)]=(\sum_{i=1}^{N}a_i\lambda_i)\tau$ and $\mathrm{Var}[n(\tau)]=(\sum_{i=1}^{N}a_i^2\lambda_i)\tau$.

Appendix D

Derivation of the Fokker-Planck equation

There are various routes to deriving the conventional Fokker-Planck equation. The earliest was described by Andrei Kolmogorov in his seminal "*On Analytical Methods in the Theory of Probability*". Below I follow the simple argument given in [Hottovy, 2011] but, for more technical treatments, I refer the reader to [Bharucha-Reid, 1960, Doob, 1953, Risken, 1989].

Consider a Markov (diffusion) process $X(t)$ with probability density $p(x,t) := p(x(t))$. Since this process is Markov, it obeys the Chapman-Kolmogorov equation [Bharucha-Reid, 1960]:

$$p(x(t_3) = x_3|x(t_1) = x_1) = \int p(x(t_3) = x_3|x(t_2) = x_2)p(x(t_2) = x_2|x(t_1) = x_1)dx_2, \quad \text{(D.1)}$$

for any $t_3 > t_2 > t_1$. This is simply implementing conditional probability and integrating over all possible intermediate steps from x_1 to x_3. Consider the evolution of the process from some invariant initial point, $X(0) = X$. We consider the integral

$$I = \int_{-\infty}^{\infty} f(Y)\frac{\partial}{\partial t}p(Y,t|X)dY, \quad \text{(D.2)}$$

where $f(Y)$ is a smooth function with compact support. The time derivative of p is then well defined as the limit

$$\lim_{\Delta t \to 0} \frac{p(Y,t+\Delta t)|X) - p(Y,t|X)}{\Delta t}$$

which can be substituted into the integral. We implement the Chapman-Kolmogorov equation, using Z as the intermediate step. Equation (D.2) is then

$$I = \lim_{\Delta t \to 0} \frac{1}{\Delta t} \left(\int_{-\infty}^{\infty} f(Y) \int_{-\infty}^{\infty} p(Y, t + \Delta t | Z, t + \frac{\Delta t}{2}) p(Z, t + \frac{\Delta t}{2} | X) dZ dY - \int_{-\infty}^{\infty} f(Y) p(Y, t|X) dY \right).$$

The second term is now solely a function of X and t, as Y is being integrated out. We can then just as well perform this integral with respect to Z. We can also re-order the integrals in the first term of the above expression, integrating with respect to Y first, and then Z, obtaining

$$= \lim_{\Delta t \to 0} \frac{1}{\Delta t} \left(\int_{-\infty}^{\infty} p(Z, t + \frac{\Delta t}{2} | X) \int_{-\infty}^{\infty} p(Y, t + \Delta t | Z, t + \frac{\Delta t}{2}) f(Y) dY dZ - \int_{-\infty}^{\infty} f(Z) p(Z, t|X) dZ \right)$$

We now make the reasonable approximation that $p(Z, t + \frac{\Delta t}{2}|X) \approx p(Z, t|X)$, which will be increasingly accurate in the limit, and apply this to the first term. This gives us the approximate expression where the two terms share a common factor. We also make use of the fact that the integral of any probability over the real line is 1, hence $f(Z) = \int_{-\infty}^{\infty} p(Y, t|Z, t + \frac{\Delta t}{2}) f(Z) dY$. Substituting this into term two for $f(Z)$, we obtain

$$I \approx \lim_{\Delta t \to 0} \frac{1}{\Delta t} \left(\int_{-\infty}^{\infty} p(Z, t|X) \int_{-\infty}^{\infty} p(Y, t + \Delta t | Z, t + \frac{\Delta t}{2}) (f(Y) - f(Z)) dY dZ \right).$$

f, being sufficiently smooth, can be expanded around Z, namely $f(Y) = f(Z) + \sum_{n=1}^{\infty} f^{(n)}(Z) \frac{(Y-Z)^n}{n!}$. Substituting this gives

$$I \approx \lim_{\Delta t \to 0} \frac{1}{\Delta t} \left(\int_{-\infty}^{\infty} p(Z, t|X) \int_{-\infty}^{\infty} p(Y, t + \Delta t | Z, t + \frac{\Delta t}{2}) \sum_{n=1}^{\infty} f^{(n)}(Z) \frac{(Y - Z)^n}{n!} dY dZ \right).$$

Defining the n^{th}-order function

$$D^{(n)}(Z, t) := \lim_{\Delta t \to 0} \frac{1}{\Delta t n!} \int_{-\infty}^{\infty} (Y - Z)^n p(Y, t + \Delta t | Z, t + \frac{\Delta t}{2}) dY,$$

we can write our original integral (now ignoring the approximation) as:

$$\int_{-\infty}^{\infty} f(Y) \frac{\partial p(Y, t|X)}{\partial t} dY = \int_{-\infty}^{\infty} p(Z, t|X) \sum_{n=1}^{\infty} f^{(n)}(Z) D^{(n)}(Z, t) dZ \tag{D.3}$$

Applying integration by parts n times to the right hand side, we have

$$\int_{-\infty}^{\infty} f(Y)\frac{\partial p(Y,t|X)}{\partial t}dY = \sum_{n=1}^{\infty}\left[\sum_{\rho=1}^{n}(-\frac{\partial}{\partial z})^{\rho-1}[p(Z,t|X)D^{(n)}(Z,t)]f^{(n-\rho)}(Z)|_{-\infty}^{\infty}+ \int_{-\infty}^{\infty}(-\frac{\partial}{\partial z})^{n}[p(Z,t|X)D^{(n)}(Z,t)]f(Z)dZ\right].$$

The series

$$\sum_{\rho=1}^{n}(-\frac{\partial}{\partial z})^{\rho-1}[p(Z,t|X)D^{(n)}(Z,t)]f^{(n-\rho)}(Z)|_{-\infty}^{\infty} = 0$$

for all n because, $p(Z,t|X)$ is a probability density function in Z so it (and its higher order derivatives) vanish at $-\infty$ and ∞. Hence we have that

$$\int_{-\infty}^{\infty} f(Y)\frac{\partial p(Y,t|X)}{\partial t}dY = \sum_{n=1}^{\infty}\int_{-\infty}^{\infty}(-\frac{\partial}{\partial z})^{n}[p(Z,t|X)D^{(n)}(Z,t)]f(Z)dZ \tag{D.4}$$

and, assuming the integrands are equal,

$$\frac{\partial p(Z,t|X)}{\partial t} = \sum_{n=1}^{\infty}(-\frac{\partial}{\partial z})^{n}[p(Z,t|X)D^{(n)}(Z,t)]. \tag{D.5}$$

Looking at the definition of $D^{(n)}(Z,t)$ carefully, you will notice that this is in fact just the definition of the n^{th} *infinitesimal* moment of the distribution $p(Y,t|Z)$. The Fokker-Planck equation is the restriction of this equation to the case where all moments higher than $n = 2$ are zero. If we re-label $D^{(1)}(Z,t) =: \mu(Z,t)$ and $D^{(2)}(Z,t) =: \frac{\sigma^2(Z,t)}{2}$, we have the conventional Fokker-Planck equation:

$$\frac{\partial p(Z,t|X)}{\partial t} = -\frac{\partial}{\partial z}[\mu(Z,t)p(Z,t|X)] + \frac{\partial^2}{\partial z^2}[\frac{\sigma^2(Z,t)}{2}p(Z,t|X)]. \tag{D.6}$$

In most cases, the underlying Langevin equation is such that the mean and variances of the random variable are independent of the random variable, as is the as is the case for the stationary-states of the Brunel and Gewaltig models.

Appendix E

Description of Simulations

Simulations were performed using Neural Simulation Tool (NEST), version 2.0 [Gewaltig and Diesmann, 2007]. Simulations were executed on the University of Cape Town High Performance Computing Cluster. The table below describes all default settings for simulations. See 1.2 for a description of the single neuron membrane potential dynamics. All data was generated from networks of the formulation described here, unless otherwise stated in the text. This regime is referred to as the "canonical network".

Simulation Protocol

Let $t_0 = 0$. Here we describe the simulation protocol used by describing what happens to the network during sequential time intervals. All times are in milliseconds.

t=0 to t=200: All neurons receive input from the Poisson generator.

t=200 to t=230: Poisson Generator ceases at t=200. No spikes are recorded for 30 ms to reduce effects of transients.

t=230 to t_{END}: Spike Detector records spikes from all neurons[1].

Calculation of statistics

Global Firing Rate of Self-Sustained state is calculated by summing all spikes recorded during the simulation, dividing by the total number of neurons and dividing by [`SimTim` −

[1]Note that, in nest, Spike Detectors cannot collect any spikes which occur in the last Δt of the simulation.

230.1]:

$$\langle \nu \rangle = \frac{Total\ Spike\ Count}{N \cdot (\texttt{SimTim} - 230.1)}$$

Variance in Firing Rate of Self-Sustained State is calculated by binning all spikes into 3 ms bins and calculating mean firing rate of each bin as above. The variance in the global rate is then the variance in the set of all 3 ms bins.

Survival Time of Self-Sustained State is calculated as $t_{\texttt{last}} - 230.1$, where $t_{\texttt{last}}$ is the time of the last recorded spike.

Inter-Spike-Intervals are calculated for each neuron. If a neuron had a total of n spikes at times t_i where $i = 1, 2, 3 \ldots, n$ and $t_1 < t_2 < t_3 < \ldots < t_n$, then it will have $n - 1$ ISI values, calculated as $t_i - t_{i-1}$ for $i = 2, \ldots, n$.

The average ISI is calculated as the average of all ISIs and the variance is similarly the variance in the set of all ISIs. These values are then used to calculate the CV for each individual simulation.

Model Summary	
Neuron Model	`iaf_psc_alpha`
Incremental time step (Δt)	0.1 ms
Simulation Duration (`SimTim`)	varied
Synaptic Current	$I_{syn} = J\frac{e}{\tau'} \cdot t \cdot \mathrm{Exp}(-\frac{t}{\tau'})$
Synaptic Time Constant (τ')	0.5 ms
Threshold Potential (V_θ)	10 mV
Resting Membrane Potential (V_E)	0 mV
Membrane time constant (τ)	30 ms
Membrane Capacitance	1 pF
Reset Membrane Potential (V_r)	0 mV
Duration of Recovery Period (τ_{rp})	2 ms
Number of Excitatory Neurons (`ExcPop`)	10 000
Number of inhibitory neurons (`ExcPop`)	2 500
Total Number of neurons (`TotPop`)	12 500
Recurrent Excitatory connections *into* each neuron (C_E)	1 000
Recurrent Inhibitory connections *into* each neuron (C_I)	250
Delay, (D)	1.5 ms
Connection weight (J)	0.1 mV
Inhibitory gain (g)	5
Doping strength (α)	40
Doped fraction (f)	$0.005 - 0.02$ (see text)
Poisson Generator (`PosGen`) (rate: ν_{ext})	$3 \times \frac{V_\theta}{\tau J C_E} = 3.33$ Hz
Spike Detector (`SpkDet`)	All 12500 neurons sampled
Connectivity	
Connection Pattern	**Applied to each neuron** (labelled i)
`RandomConvergentConnect`	`ExcPop` $\rightarrow i$: $C_E \times (1-f)$ connections, weight J
`RandomConvergentConnect`	`ExcPop` $\rightarrow i$: $C_I \times (1-f)$ connections, weight $-gJ$
`RandomConvergentConnect`	`ExcPop` $\rightarrow i$: $C_E \times f$ connections, weight αJ
`RandomConvergentConnect`	`ExcPop` $\rightarrow i$: $C_I \times f$ connections, weight $-g\alpha J$
`DivergentConnect`	`PoisGen` $\rightarrow i$: C_E connections, weight J
`ConvergentConnect`	`TotPop` $\rightarrow$ `SpkDet`

TABLE E.1: Description of Simulations. The table denotes all objects defined in the NEST simulations and all the parameter values which do not appear in the text.

Bibliography

[Abeles, 1982] Abeles, M. (1982). Role of cortical neuron: integrator or coincidence detector? *Israel Journal of Medical Science*, 18:83–92.

[Amit and Brunel, 1997] Amit, D. J. and Brunel, N. (1997). Model of global spontaneous activity and local structured activity during delay periods in the cerebral cortex. *Cerebral cortex*, 7(3):237–52.

[Amit and Tsodyks, 1991] Amit, D. J. and Tsodyks, M. (1991). Quantitative study of attractor neural network retrieving at low spike rates: I. Substrate-spikes, rates and neuronal gain. *Network: Computation in neural ...*, 2:259–273.

[Arbib, 2003] Arbib, M. A., editor (2003). *The handbook of brain theory and neural networks*. MIT Press, second edition.

[Ashby et al., 1962] Ashby, W. R., Von Foerster, H., and Walker, C. C. (1962). Instability of pulse activity in a net with threshold. *Nature*, 196:561–562.

[Barbieri and Brunel, 2008] Barbieri, F. and Brunel, N. (2008). Can attractor network models account for the statistics of firing during persistent activity in prefrontal cortex ? 2(1):114–122.

[Bertschinger and Natschläger, 2004] Bertschinger, N. and Natschläger, T. (2004). Real-time computation at the edge of chaos in recurrent neural networks. *Neural computation*, 16(7):1413–36.

[Beurle, 1956] Beurle, R. L. (1956). Properties of a mass of cells capable of regenerating pulses. *Philosophical Transactions of the Royal Society of London. Series B, BiologicalSciences*, 240(669):55–94.

[Bharucha-Reid, 1960] Bharucha-Reid, A. T. (1960). *Elements of the theory of Markov Processes and their applications*. McGraw-Hill.

[Braitenberg and Schütz, 1998] Braitenberg, V. and Schütz, A. (1998). *Cortex: statistics and geometry of neuronal connectivity*. Springer, Berlin, 2 edition.

[Brunel, 2000] Brunel, N. (2000). Dynamics of sparsely connected networks of excitatory and inhibitory spiking neurons. *Journal of computational neuroscience*, 8(3):183–208.

[Compte et al., 2000] Compte, A., Compte, A., Brunel, N., Brunel, N., Goldman-Rakic, P. S., Goldman-Rakic, P. S., Wang, X. J., and Wang, X. J. (2000). Synaptic mechanisms and network dynamics underlying spatial working memory in a cortical network model. *Cerebral cortex (New York, N.Y. : 1991)*, 10:910–23.

[Compte et al., 2003] Compte, A., Constantinidis, C., Tegner, J., Raghavachari, S., Chafee, M. V., Goldman-Rakic, P. S., and Wang, X.-J. (2003). Temporally irregular mnemonic persistent activity in prefrontal neurons of monkeys during a delayed response task. *Journal of neurophysiology*, 90:3441–3454.

[Darling and Siegert, 1953] Darling, D. A. and Siegert, A. J. F. (1953). The first passage problem for a continuous markov process. *The Annals of Mathematical Statistics*, 24(4):624–639.

[Doob, 1953] Doob, J. (1953). *Stochastic Processes*. John Wiley and Sons.

[Frolov and Medvedev, 1986] Frolov, A. A. and Medvedev, A. V. (1986). Substantiation of the 'point approximation' for describing the total electrical activity of the brain with the use of a simulation model. *Biophysics*, 31:332–337.

[Gerstner and Kistler, 2002] Gerstner, W. and Kistler, W. M. (2002). *Spiking Neuron Models: Single neurons, populations, plasticity*. Camebridge University Press.

[Gerstner et al., 2012] Gerstner, W., Sprekeler, H., and Deco, G. (2012). Theory and Simulation in Neuroscience. *Science*, 338:60–65.

[Gewaltig, 2013] Gewaltig, M. (2013). Self-sustained activity, bursts, and variability in recurrent networks. pages 1–39.

[Gewaltig and Diesmann, 2007] Gewaltig, M. and Diesmann, M. (2007). Nest (neural simulation tool). *Scholarpedia*, 2(4):1430.

[Griffith, 1963] Griffith, J. S. (1963). On the stability of brain-like structures. *Biophysical Journal*, 3:229–308.

[Grytskyy et al., 2013] Grytskyy, D., Tetzlaff, T., Diesmann, M., and Helias, M. (2013). A unified view on weakly correlated recurrent networks. *Frontiers in Computational Neuroscience*, 7(131).

[Hottovy, 2011] Hottovy, S. (2011). The fokker-planck equation. *Unpublished*.

[Inordunatum, 2013] Inordunatum (2013). Fokker-planck equation for a jump diffusion process. *Inordunatum Wordpress*.

[Knoblauch et al., 2012] Knoblauch, A., Hauser, F., Gewaltig, M.-O., Körner, E., and Palm, G. (2012). Does spike-timing-dependent synaptic plasticity couple or decouple neurons firing in synchrony? *Frontiers in Computational Neuroscience*, 6(55).

[Kopp, 2011] Kopp, E. (2011). *From Measures to Itô Integrals*. Cambridge University Press.

[Kriener et al., 2014] Kriener, B., Enger, H., Tetzlaff, T., Plesser, H. E., Gewaltig, M.-O., and Einevoll, G. T. (2014). Dynamics of self-sustained asynchronous-irregular activity in random networks of spiking neurons with strong synapses. *Front. Comp. Neurosci.*, 8(136).

[Laing, 2014] Laing, C. R. (2014). Numerical Bifurcation Theory for High-Dimensional Neural Models. *The Journal of Mathematical Neuroscience*, 4:13.

[Latham et al., 2000] Latham, P. E., Richmond, B. J., Nelson, P. G., and Nirenberg, S. (2000). Intrinsic dynamics in neuronal networks. I. Theory. *Journal of neurophysiology*, 83(2):808–27.

[Levina et al., 2007] Levina, A., Herrmann, J., and Geisel, T. (2007). Dynamical synapses causing self-organized criticality in neural networks. *Nature physics*.

[Markram et al., 2012] Markram, H., Gerstner, W., and Sjöström, P. J., editors (2012). *Spike-Timing Dependent Plasticity : A Comprehensive Overview*.

[Mitry et al., 2013] Mitry, J., McCarthy, M., Kopell, N., and Wechselberger, M. (2013). Excitable neurons, firing threshold manifolds and canards. *Journal of mathematical neuroscience*, 3(1):12.

[Mountcastle, 1957] Mountcastle, V. B. (1957). Modality and topographic properties of single neurons of cat's somatic sensory cortex. *Journal of Neurophysiology*, 20(4):408–434.

[Ostojic, 2014] Ostojic, S. (2014). Two types of asynchronous activity in networks of excitatory and inhibitory spiking neurons. *Nature neuroscience*, 17(4):594–600.

[Ostojic et al., 2009] Ostojic, S., Brunel, N., and Hakim, V. (2009). How connectivity, background activity, and synaptic properties shape the cross-correlation between spike trains. *The Journal of Neuroscience*, 29(33):10234–10253.

[Public, 2014] Public (2014). Perceptron. *Wikipedia*.

[Renart et al., 2007] Renart, A., Moreno-Bote, R., Wang, X.-J., and Parga, N. (2007). Mean-driven and fluctuation-driven persistent activity in recurrent networks. *Neural computation*, 19(1):1–46.

[Risken, 1989] Risken, H. (1989). *The Fokker-Planck Equation: Methods of Solution and Applications*. Springer-Verlag, second edition.

[Scott, 2002] Scott, A. (2002). *Neuroscience - a mathematical primer*. Springer-Verlag, New York.

[Song et al., 2005] Song, S., Sjöström, P. J., Reigl, M., Nelson, S., and Chklovskii, D. B. (2005). Highly nonrandom features of synaptic connectivity in local cortical circuits. *PLOS Biology*, 3(3):e68.

[Stein, 1965] Stein, R. B. (1965). A theoretical analysis of neuronal variability. *Biophysical Journal*, 5(2):173 – 194.

[Stein, 1967] Stein, R. B. (1967). Some models of neuronal variability. *Biophysical Journal*, 7(1):37 – 68.

[Strogatz, 1994] Strogatz, S. H. (1994). *Nonlinear Dynamics and Chaos*. Addison-Wesley Publishing Company.

[Sussillo et al., 2007] Sussillo, D., Toyoizumi, T., and Maass, W. (2007). Self-tuning of neural circuits through short-term synaptic plasticity. *Journal of neurophysiology*.

[Tao, 2011] Tao, T. (2011). An introduction to measure theory. *Online*.

[Tchumatchenko et al., 2010] Tchumatchenko, T., Malyshev, A., Geisel, T., Volgushev, M., and Wolf, F. (2010). Correlations and synchrony in threshold neuron models. *Phys. Rev. Lett.*, 104:058102.

[Torres and Kappen, 2013] Torres, J. J. and Kappen, H. J. (2013). Emerging phenomena in neural networks with dynamic synapses and their computational implications. *Frontiers in Computational Neuroscience*, 7(30).

[Tsodyks et al., 1998] Tsodyks, M., Pawelzik, K., and Markram, H. (1998). Neural networks with dynamic synapses. *Neural computation*, pages 821–835.

[Tuckwell, 1976] Tuckwell, H. C. (1976). On the First-Exit Time Problem for Temporally Homogeneous Markov Processes. *Journal of Applied Probability*, 13(1):39–48.

[Tuckwell, 1988] Tuckwell, H. C. (1988). *Introduction to theoretical neurobiology: volume 2*. Cambridge University Press.

[Vreeswijk and Sompolinsky, 1996] Vreeswijk, C. V. and Sompolinsky, H. (1996). Chaos in Neuronal Networks with Balanced Excitatory and Inhibitory Activity. *Science*, 274(5293):1724–1726.

[Vreeswijk and Sompolinsky, 1998] Vreeswijk, C. V. and Sompolinsky, H. (1998). Chaotic Balanced State in a Model of Cortical Circuits 1 Introduction. *Neural Computation*, 10:1321–1371.

[Wilson and Cowan, 1973] Wilson, H. R. and Cowan, J. D. (1973). A mathematical theory of the functional dynamics of cortical and thalamic nervous tissue. *Kybernetik*, 13(2):55–80.